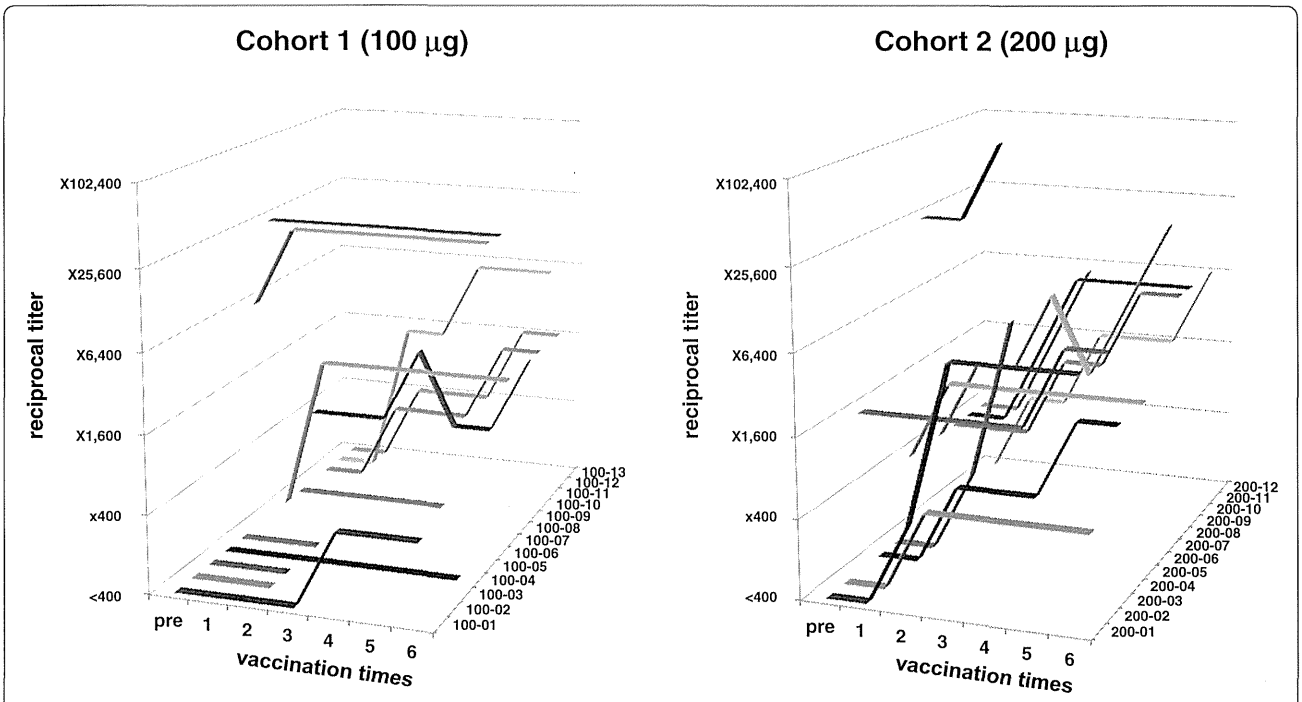

Figure 1 Antibody responses to recombinant NY-ESO-1 protein as determined by ELISA. Sera from 13 patients in Cohort 1 (100-μg dose) and 12 patients in Cohort 2 (200-μg dose) were collected at each vaccination, and serially diluted by 400, 1,600, 6,400, 25,600 and 102,400. Reciprocal titers were determined based on the maximally diluted sera, which showed a higher OD (optical density of 450–500) value than the cut-off level for NY-ESO-1 antibody positivity.

The disease progression-free survival time was 11 weeks on average, with a median of 6 weeks and range of 4 to 52 weeks. In Cohort 1 (n = 13), patients who were vaccinated with 100 μg of CHP-NY-ESO-1 survived without disease progression for 11 weeks on average, with a median of 6 weeks and range of 4 to 52 weeks. In Cohort 2 (n = 12) in which patients received the 200-μg dose, the patients were progression-free for 10 weeks on average, with a median of 8.5 weeks and range of 6 to 18 weeks (Table 4). There was no difference between the two cohorts (p = 0.748, Figure 2-A).

The overall survival time was 33 weeks on average, with a median of 31 weeks and range of 4 to 72 weeks. In Cohort 1 (n = 13), the patients survived for 25 weeks on average, with a median of 23 weeks and range of 4 to 60 weeks. In Cohort 2 (n = 12), they survived for 41 weeks on average, with a median of 41 weeks and range of 8 to 72 weeks (Table 4). The patients vaccinated with 200 μg of CHP-NY-ESO-1 had statistically longer survival than those who received the 100-μg dose (p = 0.050, Figure 2-B). Each cohort included three patients who were vaccinated three times or less because of early disease progression, and were withdrawn from this study, respectively. Having excluded those 6 patients, the patients vaccinated with 200 μg-vaccine still had longer survival than those with 100 μg-vaccinations (data not shown).

When the survival of patients who had responded to previous therapies (n = 12) was compared to non-responders (n = 13), the responders lived longer than the non-responders after vaccination (p = 0.005, Figure 2-C). The patients who never responded to previous therapies and received the 200-μg dose (n = 6) significantly lived longer than those who received the 100-μg dose (n = 7) (p = 0.029, Figure 2-D).

When the survival of patients who had tumors with a maximal diameter of 30 mm or less, including non-measurable lesions (n = 13) was compared with those with diameters more than 30 mm (n = 12), the patients with higher tumor burdens had shorter life spans (p = 0.021, Figure 2-E). Among patients with higher tumor burdens, patients who were vaccinated with the 200-μg dose (n = 4) lived longer than those who received the 100-μg dose (n = 8), (p = 0.037, Figure 2-F).

Using Cox proportional hazards models, the vaccine dose and the responsiveness to previous therapy were independent factors that influenced the overall survival, which showed p = 0.011 with HR 3.595 (95%CI 1.335-9.678) and p = 0.002 with HR 0.194 (95%CI 0.068-0.553), respectively. Also, the vaccine dose and the tumors sizes including non-measurable disease independently affected the overall survival, showing p = 0.040 with HR 2.630 (95%CI 1.045-6.614) and p = 0.020 with HR 0.322 (95%CI 0.124-0.833), respectively.

Table 4 Baseline clinical profiles and responses after CHP-NY-ESO-1 vaccinations

100 μg						200 μg					
pt No.	Response to previous therapies (duration time, weeks)	*sum of tumor diameters (mm)	Tumor response (BOR)	Time-to-progression (weeks)	Survival (weeks)	pt No.	Response to previous therapies (duration time, weeks)	*sum of tumor diameters (mm)	Tumor response (BOR)	Time-to-progression (weeks)	Survival (weeks)
100-01	PR (4)	NA	PD	6	31	200-01	PR (29)	24	SD	17	70
100-02	SD	53	NE	4	6	200-02	NE	25	SD	18	33
100-03	NE	144	NE	4	6	200-03	PR (32)	55	PD	6	37
100-04	PD	182	PD	5	17	200-04	PR (30)	NA	PD	6	50
100-05	CR (38)	101	NE	4	4	200-05	PR (32)	NA	PD	6	72
100-06	SD	69	PD	6	31	200-06	NE	32	SD	18	54
100-07	CR (15)	78	PD	6	29	200-07	NE	205	NE	6	8
100-08	NE	39	SD	18	23	200-08	PR (12)	16	SD	11	33
100-09	SD	18	PD	6	8	200-09	CR (96)	88	PD	6	45
100-10	CR (24)	NA	SD	11	60	200-10	SD	NA	SD	12	48
100-11	SD	31	SD	12	20	200-11	SD	NA	NE	6	12
100-12	PR (9)	NA	NE	16	28	200-12	SD	NA	SD	12	33
100-13	PR (16)	NA	NE	52	59						

*target lesions determined based on RECIST criteria.

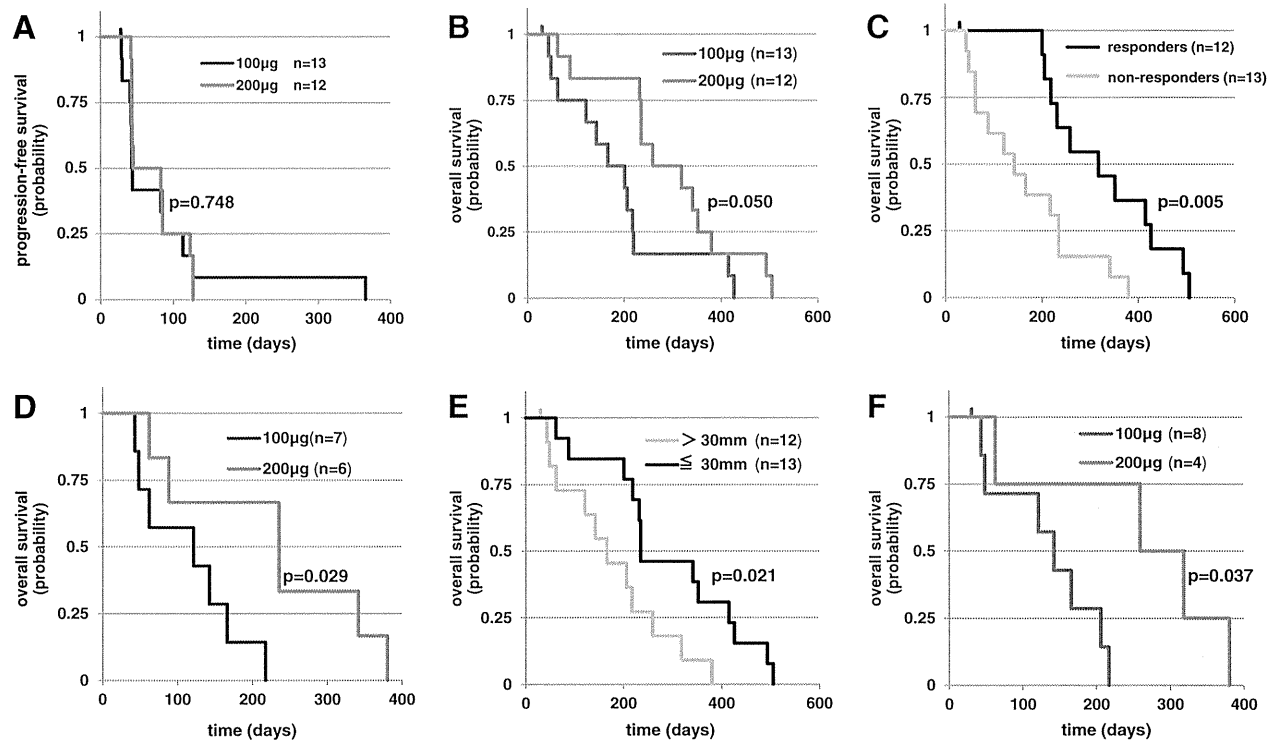

Figure 2 Kaplan-Meier survival curves of patients who were alive after the CHP-NY-ESO-1 vaccinations. A: Progression-free survival (PFS) of patients assigned to Cohort 1 (100-μg dose, n = 13) or Cohort 2 (200-μg dose, n = 12). The probability of PFS of the patients who received 200 μg of the vaccine and those who received the 100-μg dose were similar (log-rank test, p = 0.748). **B**: Overall survival (OS) of patients assigned to Cohort 1 or Cohort 2. The patients who received 200 μg of the vaccine survived longer than those who received the 100-μg dose. (log-rank test, p = 0.050). **C**: OS of patients vaccinated with either 100 μg or 200 μg of CHP-NY-ESO-1 compared between patients who responded to previous therapies and those who never responded. The patients who responded to previous therapies and were vaccinated with CHP-NY-ESO-1 survived longer than non-responders. (log-rank test, p = 0.0050). **D**: OS of patients vaccinated with 100 μg or 200 μg of CHP-NY-ESO-1 who never responded to previous therapies. The patients who received 200 μg of the vaccine survived longer than those who received the 100-μg dose (log-rank test, p = 0.029). **E**: OS of patients vaccinated with 100 μg or 200 μg of CHP-NY-ESO-1 compared with either baseline tumor burdens of >30 mm (sum of the tumor diameters) or 30 mm or less including non-measurable lesions. The patients with a tumor burden higher than 30 mm had reduced survival compared to those with smaller burdens (log-rank test, p = 0.021). **F**: OS of patients who received 100 μg or 200 μg of CHP-NY-ESO-1 who had baseline tumor burdens greater than 30 mm. The patients who received 200 μg of the vaccine survived longer than those who received the 100-μg dose (log-rank test, p = 0.037).

This study was a phase 1 dose-escalating clinical trial that examined two doses of the CHP-NY-ESO-1 vaccine in esophageal cancer patients. The primary goals were to evaluate the vaccine safety and immune responses to the NY-ESO-1 antigen, and we further explored the clinical effects on esophageal cancer patients with a poor prognosis.

CHP consists of a hydrophobic polysaccharide pullulan containing chemically introduced cholesterol groups, which spontaneously aggregate to form nano-sized particles that can contain antigen proteins. Using this system as a vaccine, tumor antigen proteins delivered to antigen-presenting cells can stimulate both antigen-specific CD4+ T cells and CD8+ T cells. In a pre-clinical study, dendritic cells pulsed with the CHP-NY-ESO-1 complex could induce both NY-ESO-1-specific CD4+ and CD8+ T cells [4]. Previous clinical studies using CHP-HER2 and CHP-NY-ESO-1 vaccines have shown that these vaccines can induce antigen-specific $CD4^+$ and $CD8^+$ T cell immunity in cancer patients [5-7].

In the current study, we found that CHP-NY-ESO-1 was clinically safe and that the immune responses to the NY-ESO-1 antigen, which were evaluated based on IgG antibody titers, showed a dose-dependent effect between the 100-μg dose and 200-μg. Furthermore, the survival rates of patients who were vaccinated with the 200-μg dose were superior to those who received the 100-μg dose. The patients had recurrent or metastatic esophageal tumors that exhibited clinical resistance to chemotherapy or radiotherapy. The first 13 patients were enrolled to Cohort 1, and the next 12 patients were included in Cohort 2. As the clinical backgrounds of the two cohorts were similar, it was reasonable to make a comparative consideration.

As the previous NY-ESO-1 protein vaccine trials have demonstrated, the toxicity of the CHP-vaccine was very

mild. Grade 3 swallowing disturbances were seen, which were likely related to the progression of esophageal cancer. The other grade 3 events included diarrhea, which was not related to the vaccine. The only related events were grade 1 skin reactions at the injection sites.

Previous vaccine trials have used recombinant full-length NY-ESO-1 protein with various adjuvants. Melanoma patients were divided into three cohorts that were vaccinated with 10 μg, 30 μg or 100 μg of the NY-ESO-1 protein in combination with the saponin adjuvant ISCOMATRIX [10]. The 100-μg dose of NY-ESO-1 induced more immune responses than the other two doses. The responses were evaluated based on IgG antibody titers and delayed-type hypersensitivity (DTH) of skin reactions. In the CHP system, a single 100-μg dose of CHP-NY-ESO-1 was examined with or without the adjuvant OK-432 [6,7,16]. These reports suggested that the 100-μg dose of CHP-NY-ESO-1 is sufficient to induce immune responses. The current trial was designed to determine whether the NY-ESO-1 protein vaccine has potential dose-dependent effects on immunogenicity in patients with homogeneous backgrounds. By assessing humoral immune responses in the cohorts that received 100 μg and 200 μg of the vaccine, the responses appeared in the early phases. We initially intended to analyze antibodies using samples from patients who were vaccinated for at least 4 cycles, as we thought it could take at least 4 cycles to detect immune responses. In the overall data acquisition, samples from all 25 patients were analyzed, which included sera from at least two vaccinations. In conclusion, we found that the 200-μg dose was more efficient than the 100-μg dose.

The other reports included vaccine studies using recombinant NY-ESO-1 protein in combination with Imiquimod and CpG [17,18]. In these studies, the NY-ESO-1 protein was given at doses of 100 μg, and 100 μg or 400 μg, respectively. Based on the patients' sera, the 400-μg dose might have induced more antibody responses than the 100-μg dose, but this was not statistically analyzed. Combined with these reports, the NY-ESO-1 protein might be immunogenic at increasing doses of 10 μg, 30 μg, 100 μg and 200 μg. Since dose-limited toxicity (DLT) was not observed at the higher dose of 200 μg in this study, additional dose increments might be acceptable to determine whether higher doses can induce stronger immune responses.

In this study, we explored a long-term clinical outcome of the NY-ESO-1 protein vaccine. This study was not initially designed to detect a statistical significance of the clinical effect between the 2 cohorts. Instead, we made a comparison to find out if there might include a positive signal for further clinical trials of this vaccine. The NY-ESO-1 protein vaccine with the adjuvant ISCOMATRIX suggested that melanoma patients who were vaccinated after standard therapy tended to have fewer relapses [10], which were not statistically analyzed. The other studies reported that vaccinations with NY-ESO-1-expressing poxvirus vectors and NY-ESO-1 overlapping peptides both prolonged progression-free survivals in ovarian cancer patients who did not have measurable disease after standard therapy [19,20]. In this study, most of the patients developed disease-progression in 6 months, and there was no difference between the patients vaccinated with 100 μg and 200 μg of the CHP-NY-ESO-1, as the previous studies demonstrated that disease-progression occurs in the early phase of vaccinations [12,21].

In contrast, we found that dose-dependent effects of the CHP-NY-ESO-1 vaccine on overall survival of patients with advanced/metastatic esophageal cancer. Analyzing other clinical categories, both the baseline tumor sizes and the tumor responsiveness to previous therapies were significant factors influencing the overall survival. Using Cox proportional hazards models, it was indicated that the tumor sizes and the vaccine doses independently influenced the survival. In the same way, the responsiveness to previous therapies and the vaccine doses independently affected the survival. Therefore, it is suggested that the higher dose of CHP-NY-ESO-1 vaccine played a role in prolongation of the overall survival in the esophageal cancer patients.

In addition, the higher-dose of the vaccine provided significant survival benefit in patients who never responded to the previous therapies or had larger tumor burdens than the lower dose vaccinations. It is difficult to discuss why the patients with a poorer prognosis were more benefited from the 200-μg dose of the vaccine than 100-μg. It might be speculated that the dose-dependency clinical benefits were more often observable in patients with a poorer prognosis, because they might have needed more immune responses in order to survive longer by preventing disease deterioration.

In the previous CHP-NY-ESO-1 vaccine study, which was a phase 1 study that enrolled various types of NY-ESO-1-expressing cancer patients, tumor regression was observed in two out of four esophageal cancer patients [6]. However, tumor shrinkage is rarely observed in cancer vaccine therapies, although some disease stabilization is seen. This study shows that clinical benefits, such as long-term survival, can be detected if a clinical trial is designed in a comparative way. The results were not compared to unvaccinated controls, and it is not possible to directly determine the effects of the vaccine, but is possible to reasonably interpret the effects of immune response on the clinical outcomes.

Conclusions

The safety and immunogenicity of the CHP-NY-ESO-1 vaccine were confirmed in the patients with antigen-expressing esophageal cancer. The 200-μg dose efficiently induced antigen-specific immune responses and suggested better survival benefits, even for patients with a poorer prognosis. In future clinical trials, 200 μg will be the recommended dose.

Abbreviations
BOR: Best overall response; NA: Not available; NE: Not evaluable.

Competing interests
This study is supported by ImmunoFrontier, Inc. and Naozumi Harada is an employee, and Mami Ohnishi and Tadashi Hishida are former employees of ImmunoFrontier, Inc. Hiroshi Shiku is a stockholder of ImmunoFrontier, Inc.

Authors' contributions
SK, HW, KM, YN, SU, HM, ST and YD treated patients and provided the clinical data. SHS and YM worked on immune responses. HI, NI and ES evaluated tumor antigen expression. TY, MOs and MOh worked on the study statistics. NH and TH were responsible for manufacturing the study drug. SK and HS wrote the manuscript. All authors read and approved the final manuscript.

Acknowledgements
We thank all co-workers from all units of Osaka University Hospital, Mie University Hospital, Kitano Hospital and Aichi Cancer Center Hospital for their skills in making this trial run successfully and for the support they provided to the patients under their care. We also thank all co-workers from FiveRings, Co. Ltd. and Statcom Co. Ltd. for operating and analyzing this study. We express thanks to Mr. Masanobu Kimura, Dr. Keigo Hanada (ImmunoFrontier, Inc.) and Mr. Hiroshi Miyamoto (FiveRings, Co. Ltd.) for their special contributions to operating this clinical trial.

Author details
[1]Departments of Immuno-Gene Therapy and Cancer Vaccine, Mie University Graduate School of Medicine, 2-174, Edobashi, Tsu, Mie 514-8507, Japan. [2]Department of Gastroenterological Surgery, Osaka University Graduate School of Medicine, Yamadaoka 2-2 (E2), Suita, Osaka 565-0871, Japan. [3]Department of Clinical Oncology, Aichi Cancer Center Hospital, 1-1Kanokoden, Chikusa-ku Nagoya 464-8681, Japan. [4]Department of Endoscopy, Aichi Cancer Center Hospital, 1-1Kanokoden, Chikusa-ku Nagoya 464-8681, Japan. [5]Department of Gastroenterological Surgery and Oncology, Kitano Hospital, The Tazuke Kofukai Medical Research Institute, 2-4-20 Ohgimachi, Kita-ku, Osaka 530-8480, Japan. [6]Department of Anatomic Pathology, Tokyo Medical University, 6-1-1Shinjuku, Shinjuku-ku, Tokyo 160-8402, Japan. [7]Department of Translational Medical Science, Mie University Graduate School of Medicine, 2-174, Edobashi, Tsu, Mie 514-8507, Japan. [8]FiveRings, Co. Ltd, 9-4, 2-chome, Higashi-Tenman, Kita-ku, Osaka 530-0044, Japan. [9]ImmunoFrontier, Inc, 5-10, 2-chome, Sannou, Ota-ku, Tokyo 143-0023, Japan.

Received: 13 July 2013 Accepted: 30 September 2013
Published: 5 October 2013

References
1. Gu XG, Schmitt M, Hiasa A, Nagata Y, Ikeda H, Sasaki Y, Akiyoshi K, Sunamoto J, Nakamura H, Kuribayashi K, Shiku H: **A novel hydrophobized polysaccharide/oncoprotein complex vaccine induces in vitro and in vivo cellular and humoral immune responses against HER2-expressing murine sarcomas.** *Cancer Res* 1998, **58**:3385–3390.
2. Ikuta Y, Katayama N, Wang L, Okugawa T, Takahashi Y, Schmitt M, Gu X, Watanabe M, Akiyoshi K, Nakamura H, Kuribayashi K, Sunamoto J, Shiku H: **Presentation of a major histocompatibility complex class 1-binding peptide by monocyte-derived dendritic cells incorporating hydrophobized polysaccharide-truncated HER2 protein complex: implications for a polyvalent immuno-cell therapy.** *Blood* 2002, **99**:3717–3724.
3. Wang L, Ikeda H, Ikuta Y, Schmitt M, Miyahara Y, Takahashi Y, Gu X, Nagata Y, Sasaki Y, Akiyoshi K, Sunamoto J, Nakamura H, Kuribayashi K, Shiku H: **Bone marrow-derived dendritic cells incorporate and process hydrophobized polysaccharide/oncoprotein complex as antigen presenting cells.** *Int J Oncol* 1999, **14**:695–701.
4. Hasegawa K, Noguchi Y, Koizumi F, Uenaka A, Tanaka M, Shimono M, Nakamura H, Shiku H, Gnjatic S, Murphy R, Hiramatsu Y, Old LJ, Nakayama E: **In vitro stimulation of CD8 and CD4 T cells by dendritic cells loaded with a complex of cholesterol-bearing hydrophobized pullulan and NY-ESO-1 protein: Identification of a new HLA-DR15-binding CD4 T-cell epitope.** *Clin Cancer Res* 2006, **12**:1921–1927.
5. Kitano S, Kageyama S, Nagata Y, Miyahara Y, Hiasa A, Naota H, Okumura S, Imai H, Shiraishi T, Masuya M, Nishikawa M, Sunamoto J, Akiyoshi K, Kanematsu T, Scott AM, Murphy R, Hoffman EW, Old LJ, Shiku H: **HER2-specific T-cell immune responses in patients vaccinated with truncated HER2 protein complexed with nanogels of cholesteryl pullulan.** *Clin Cancer Res* 2006, **12**:7397–7405.
6. Uenaka A, Wada H, Isobe M, Saika T, Tsuji K, Sato E, Sato S, Noguchi Y, Kawabata R, Yasuda T, Doki Y, Kumon H, Iwatsuki K, Shiku H, Monden M, Jungbluth AA, Ritter G, Murphy R, Hoffman E, Old LJ, Nakayama E: **T cell immunomonitoring and tumor responses in patients immunized with a complex of cholesterol-bearing hydrophobized pullulan (CHP) and NY-ESO-1 protein.** *Cancer Immun* 2007, **7**:9–19.
7. Kawabata R, Wada H, Isobe M, Saika T, Sato S, Uenaka A, Miyata H, Yasuda T, Doki Y, Noguchi Y, Kumon H, Tsuji K, Iwatsuki K, Shiku H, Ritter G, Murphy R, Hoffman E, Old LJ, Monden M, Nakayama E: **Antibody response against NY-ESO-1 in CHP-NY-ESO-1 vaccinated patients.** *Int J Cancer* 2007, **120**:2178–2184.
8. Chen YT, Scanlan MJ, Sahin U, Türeci O, Gure AO, Tsang S, Williamson B, Stockert E, Pfreundschuh M, Old LJ: **A testicular antigen aberrantly expressed in human cancers detected by autologous antibody screening.** *Proc Natl Acad Sci U S A* 1997, **94**:1914–1918.
9. Jungbluth AA, Chen YT, Stockert E, Busam KJ, Kolb D, Iversen K, Coplan K, Williamson B, Altorki N, Old LJ: **Immunohistochemical analysis of NY-ESO-1 antigen expression in normal and malignant human tissues.** *Int J Cancer* 2001, **92**:856–860.
10. Davis ID, Chen W, Jackson H, Parente P, Shackleton M, Hopkins W, Chen Q, Dimopoulos N, Luke T, Murphy R, Scott AM, Maraskovsky E, McArthur G, MacGregor D, Sturrock S, Tai TY, Green S, Cuthbertson A, Maher D, Miloradovic L, Mitchell SV, Ritter G, Jungbluth AA, Chen YT, Gnjatic S, Hoffman EW, Old LJ, Cebon JS: **Recombinant NY-ESO-1 protein with ISCOMATRIX adjuvant induces broad integrated antibody and CD4(+) and CD8(+) T cell responses in humans.** *Proc Natl Acad Sci U S A* 2004, **101**:10697–10702.
11. Eisenhauer EA, Therasse P, Bogaerts J, Schwartz LH, Sargent D, Ford R, Dancey J, Arbuck S, Gwyther S, Mooney M, Rubinstein L, Shankar L, Dodd L, Kaplan R, Lacombe D, Verweij J: **New response evaluation criteria in solid tumours: revised RECIST guideline (version 1.1).** *Eur J Cancer* 2009, **45**:228–247.
12. Wolchok JD, Hoos A, O'Day S, Weber JS, Hamid O, Lebbé C, Maio M, Binder M, Bohnsack O, Nichol G, Humphrey R, Hodi FS: **Guidelines for the evaluation of immune therapy activity in solid tumors: immune-related response criteria.** *Clin Cancer Res* 2009, **15**:7412–7420.
13. Trotti A, Colevas AD, Setser A, Rusch V, Jaques D, Budach V, Langer C, Murphy B, Cumberlin R, Coleman CN, Rubin P: **CTCAE v3.0: development of a comprehensive grading system for the adverse effects of cancer treatment.** *Semin Radiat Oncol* 2003, **13**:176–181.
14. Fujita S, Wada H, Jungbluth AA, Sato S, Nakata T, Noguchi Y, Doki Y, Yasui M, Sugita Y, Yasuda T, Yano M, Ono T, Chen YT, Higashiyama M, Gnjatic S, Old LJ, Nakayama E, Monden M: **NY-ESO-1 expression and immunogenicity in esophageal cancer.** *Clin Cancer Res* 2004, **10**:6551–6558.
15. Stockert E, Jäger E, Chen YT, Scanlan MJ, Gout I, Karbach J, Arand M, Knuth A, Old LJ: **A survey of the humoral immune response of cancer patients to a panel of human tumor antigens.** *J Exp Med* 1998, **187**:1349–1354.
16. Aoki M, Ueda S, Nishikawa H, Kitano S, Hirayama M, Ikeda H, Toyoda H, Tanaka K, Kanai M, Takabayashi A, Imai H, Shiraishi T, Sato E, Wada H, Nakayama E, Takei Y, Katayama N, Shiku H, Kageyama S: **Antibody responses against NY-ESO-1 and HER2 antigens in patients vaccinated with combinations of cholesteryl pullulan (CHP)-NY-ESO-1 and CHP-HER2 with OK-432.** *Vaccine* 2009, **27**:6854–6861.
17. Adams S, O'Neill DW, Nonaka D, Hardin E, Chiriboga L, Siu K, Cruz CM, Angiulli A, Angiulli F, Ritter E, Holman RM, Shapiro RL, Berman RS, Berner N, Shao Y, Manches O, Pan L, Venhaus RR, Hoffman EW, Jungbluth A, Gnjatic S, Old L, Pavlick AC, Bhardwaj N: **Immunization of malignant melanoma patients with full-length NY-ESO-1 protein using TLR7 agonist imiquimod as vaccine adjuvant.** *J Immunol* 2008, **181**:776–784.
18. Valmori D, Souleimanian NE, Tosello V, Bhardwaj N, Adams S, O'Neill D, Pavlick A, Escalon JB, Cruz CM, Angiulli A, Angiulli F, Mears G, *et al*: **Vaccination with NY-ESO-1 protein and CpG in Montanide induces integrated antibody/Th1 responses and CD8 T cells through cross-priming.** *Proc Natl Acad Sci U S A* 2007, **104**:8947–8952.
19. Odunsi K, Matsuzaki J, Karbach J, Neumann A, Mhawech-Fauceglia P, Miller A, Beck A, Morrison CD, Ritter G, Godoy H, Lele S, Dupont N, *et al*: **Efficacy**

of vaccination with recombinant vaccinia and fowlpox vectors expressing NY-ESO-1 antigen in ovarian cancer and melanoma patients. *Proc Natl Acad Sci U S A* 2012, **109**:5797–5802.

20. Sabbatini P, Tsuji T, Ferran L, Ritter E, Sedrak C, Tuballes K, Jungbluth AA, Ritter G, Aghajanian C, Bell-McGuinn K, Hensley ML, Konner J, *et al*: **Phase I trial of overlapping long peptides from a tumor self-antigen and poly-ICLC shows rapid induction of integrated immune response in ovarian cancer patients.** *Clin Cancer Res* 2012, **18**:6497–6508.
21. Small EJ, Schellhammer PF, Higano CS, Redfern CH, Nemunaitis JJ, Valone FH, Verjee SS, Jones LA, Hershberg RM: **Placebo-controlled phase III trial of immunologic therapy with Sipuleucel-T (APC8015) in patients with metastatic, asymptomatic hormone refractory prostate cancer.** *J Clin Oncol* 2006, **24**:3089–3094.

doi:10.1186/1479-5876-11-246
Cite this article as: Kageyama *et al.*: Dose-dependent effects of NY-ESO -1 protein vaccine complexed with cholesteryl pullulan (CHP-NY-ESO-1) on immune responses and survival benefits of esophageal cancer patients. *Journal of Translational Medicine* 2013 11:246.

IJC
International Journal of Cancer

New findings of kinase switching in gastrointestinal stromal tumor under imatinib using phosphoproteomic analysis

Tsuyoshi Takahashi[1,2], Satoshi Serada[2], Maiko Ako[2], Minoru Fujimoto[2], Yasuaki Miyazaki[1], Rie Nakatsuka[1,2], Takayuki Ikezoe[3], Akihito Yokoyama[3], Takahiro Taguchi[4], Kazuki Shimada[5], Yukinori Kurokawa[1], Makoto Yamasaki[1], Hiroshi Miyata[1], Kiyokazu Nakajima[1], Shuji Takiguchi[1], Masaki Mori[1], Yuichiro Doki[1], Tetsuji Naka[2] and Toshirou Nishida[2,6]

[1] Department of Surgery, Osaka University Graduate School of Medicine, Suita, Japan
[2] Laboratory for Immune Signal, National Institute of Biomedical Innovation, Ibaraki, Japan
[3] Department of Hematology and Respiratory Medicine, Kochi Medical School, Kochi University, Nankoku, Japan
[4] Research and Education Faculty, Multidisciplinary Science Cluster, Kuroshio Science Unit, Kochi Medical School, Kochi University, Nankoku, Japan
[5] Department of Respiratory Medicine, Allergy and Rheumatic Diseases, Osaka University Graduate School of Medicine, Suita, Japan
[6] Department of Surgery, Osaka Police Hospital, Osaka, Japan

Despite the revolutionary effects of imatinib on advanced gastrointestinal stromal tumors (GISTs), most patients eventually develop disease progression following primary resistance or acquired resistance driven by secondary-resistant mutations. Even in radiographically vanishing lesions, pathology has revealed persistent viable cells during imatinib therapy, which could lead to the emergence of drug-resistant clones. To uncover the mechanisms underlying these clinical issues, here we examined imatinib-induced phosphoproteomic alterations in GIST-T1 cells, using our quantitative tyrosine phosphoproteomic analysis method, which combined immunoaffinity enrichment of phosphotyrosine-containing peptides with isobaric tags for relative and absolute quantitation (iTRAQ) technology. Using this approach, we identified 171 tyrosine phosphorylation sites spanning 134 proteins, with 11 proteins exhibiting greater than 1.5-fold increases in tyrosine phosphorylation. Among them, we evaluated FYN and focal adhesion kinase (FAK), both of which are reportedly involved in proliferation and malignant alteration of tumors. We confirmed increased tyrosine phosphorylation of both kinases by western blotting. Inhibition of FYN and FAK phosphorylation each increased tumor cell sensitivity to imatinib. Furthermore, a FAK-selective inhibitor (TAG372) induced apoptosis of imatinib-resistant GIST-T1 cells and decreased the imatinib IC_{50}. These results indicate that FYN or FAK might be potential therapeutic targets to overcome resistance to imatinib in GISTs. Additionally, we showed that the iTRAQ-based quantitative phosphotyrosine-focused phosphoproteomic approach is a powerful method for screening phosphoproteins associated with drug resistance.

The gastrointestinal stromal tumor (GIST) is the most common mesenchymal tumor of the digestive tract, and is characterized by expression of the KIT (CD117) and/or DOG1 proteins. Most GISTs have oncogenic *KIT* or *PDFGRA* mutations, which is a key factor in sporadic GIST pathogenesis and proliferation.[1–3] This knowledge has facilitated the development of targeted therapies with tyrosine kinase inhibitors and led to the revolutionary treatment with imatinib mesylate (Glivec®; Novartis Pharmaceuticals). Recent clinical trials with advanced/unresectable GIST have shown that imatinib produces objective responses in ~50% of patients, and disease stabilization (stable disease) in another 30–40%. The corresponding 2-year overall survival rates range from 70 to 80%, indicating markedly improved patient outcomes compared with anecdotal data from cytotoxic chemotherapy in the preimatinib era.[4–6]

Despite imatinib's effectiveness, there remain several problems. First, GIST patients cannot stop taking the drug even if complete response is obtained, because discontinuation inevitably leads to reprogression and disease relapse.[7,8] Second, imatinib activity is limited by primary resistance to the drug in ~15% of patients, and secondary resistance eventually develops in more than 80% of patients.[5,9] Secondary resistance mainly occurs due to additional kinase domain mutations, which are thought to develop in viable tumor cells (persistent cells) during imatinib therapy. It is not yet known

Key words: GIST, imatinib, iTRAQ, proteomics
Abbreviations: FAK: focal adhesion kinase; GIST: gastrointestinal stromal tumor; iTRAQ: isobaric tags for relative and absolute quantitation; LC: liquid chromatography; MS/MS: tandem mass spectrometry; shRNA: small hairpin RNA; siRNA: small interfering RNA
Additional Supporting Information may be found in the online version of this article.
DOI: 10.1002/ijc.28282
History: Received 17 Dec 2012; Accepted 2 May 2013; Online 28 May 2013
Correspondence to: Toshirou Nishida, Department of Surgery, Osaka Police Hospital, 10-31, Kitayama-cho, Tennoji-ku, Osaka 543-0035, Japan, Tel.: +81-6-6771-6051, Fax: +81-6-6775-2838, E-mail: toshin@mvb.biglobe.ne.jp

Int. J. Cancer: **133**, 2737–2743 (2013) © 2013 UICC

Short Report

What's new?

While the targeted tyrosine kinase inhibitor imatinib can significantly improve two-year survival rates for patients with gastrointestinal stromal tumor (GIST), primary and secondary resistance mutations often limit its benefits. This study of the human GIST-T1 cell line suggests that imatinib-induced increases in tyrosine phosphorylation of FYN kinase and focal adhesion kinase (FAK) may be responsible for mediating some instances of imatinib resistance and therefore may be potential targets for killing persistent tumor cells and overcoming resistance. The findings also indicate that iTRAQ-based quantitative phosphotyrosine-focused proteomic analysis is a useful way of screening for phosphoproteins associated with drug resistance.

what mechanisms keep these persistent cells alive after shutdown of KIT signaling by imatinib.

Phosphorylation of protein kinases in signaling pathways is a key event in tumor cell survival and proliferation. Differential phosphoprotein analysis may provide clues to alternatively activated pathways and/or substituted kinases that may be activated after inhibition of main pathways, such as KIT.[10] Recent advances in mass spectrometry-based phosphoproteomics enable extensive profiling of serine-threonine kinases, while tyrosine kinase analysis has remained challenging in terms of quantity and quality. However, a recent method coupling peptide-level antiphosphotyrosine immunoaffinity purification with liquid chromatography (LC)-tandem mass spectrometry (MS/MS) has provided reasonable profiling for tyrosine phosphorylation.[11]

In the present study, we quantitatively measured the phosphoproteomic alterations induced by imatinib in a GIST-T1 cell line. We also examined the roles of some tyrosine kinases that were activated in persistent tumor cells after imatinib exposure.

Material and Methods

Cell lines

We previously established the human GIST cell line GIST-T1, which has a 57-nucleotide (V570-Y578) in-frame deletion in KIT exon 11.[12] The cell line identity was confirmed by DNA fingerprinting through short tandem repeat profiling, as previously described.[13] GIST-T1-R was established from GIST-T1 as an imatinib-resistant clone that arose from continuous culturing in 5 μM imatinib. The GIST-T1-R cells GIST-T1-R2 and GIST-T1-R8 each exhibit imatinib IC_{50} values of ~30 μM, which is ~1000 times that of the GIST-T1 parent.

Reagents and antibodies

Imatinib and TAG372—selective tyrosine kinase inhibitors for KIT and focal adhesion kinase (FAK), respectively—were synthesized and provided by Novartis Pharmaceuticals (Basel, Switzerland). The following primary antibodies were used: anti-phospho-Src Family (Tyr416) (1:1000), anti-phospho-ERK and anti-ERK from Cell Signaling Technology (Danvers, MA); anti-GAPDH from Santa Cruz Biotechnology (Santa Cruz, CA); anti-phospho-FAK (Tyr397) from Biosource (Camarillo, CA); anti-FAK from BD Transduction Laboratories (San Jose, CA) and anti-phosphotyrosine (clone 4G10) from Upstate Biotechnology (Lake Placid, NY). Detailed immunoprecipitation information is provided in the Supporting Information Materials and Methods section.

Peptide synthesis

A tyrosine-phosphorylated peptide (NVPLyK) derived from a trypsinized peptide sequence of yeast alpha-enolase was synthesized at Sigma Aldrich (Milwaukee, WI) using standard solid-phase peptide synthesis techniques and Fmoc chemistry.

Phosphopeptide immunoprecipitation

GIST-T1 cells were treated with 400 nM of imatinib for 0, 1, 6 and 24 hr. Tyrosine-phosphorylated peptides were purified using Cell Signaling PhosphoScan pTyr100 Kits (Beverly, MA) following the manufacturer's instructions with minor modification. Detailed information is provided in the Supporting Information Materials and Methods section.

iTRAQ labeling

After immunoprecipitation, peptides were dissolved in 9.8 M Urea (5 μL) and 1 M TEAB (20 μL). Following the manufacturer's protocol (Applied Biosystems, Foster City, CA), the samples were labeled with the isobaric tags for relative and absolute quantitation (iTRAQ) reagents as follows: GIST-T1 with reagent 114 (0 hr), GIST-T1 with reagent 115 (1 hr), GIST-T1 with reagent 116 (6 hr) and GIST-T1 with reagent 117 (24 hr). The labeled peptide samples were then pooled and desalted with Sep-Pak Light C18 Cartridges, and the peptides were dried in a SpeedVac. The labeled peptide mixtures were purified and fractionated into 14 fractions using strong cation exchange fractionation, as previously described.[13]

Quantitative mass spectrometric analysis

Nano LC-MS/MS analysis and iTRAQ data analysis were performed as described in the Supporting Information Materials and Methods section.

Small interfering RNA transfection

Commercial FAK small interfering RNA (siRNA) and nonspecific siRNA were obtained from QIAGEN. Cells were transfected with siRNA using Lipofectamine 2000 reagent

(Invitrogen) following the manufacturer's instructions. Selective silencing of FAK was confirmed by western blot analysis.

Generation of FYN knockdown cells

To generate stable FYN knockdown cell lines, GIST-T1 cells were transfected with a commercial plasmid containing an anti-FYN short hairpin RNA (shRNA Fyn, plasmid KH00147N; SABiosciences [Qiagen], Frederick, MD) using Lipofectamine 2000 (Invitrogen, Carlsbad, CA) according to the manufacturer's instructions. The correctly transfected and expressing cells were selected with 600 μg/mL G418 (Invitrogen). Stable clones were maintained in 250 μg/mL G418. Three stable GIST-T1-FYN shRNA cell lines were established, designated B1, B2 and B3 cells. We also established a control cell line of GIST-T1 stably transfected with the empty vector, which we designated GIST-T1-C.

Measurement of IC_{50} after imatinib treatment

Cells were seeded in 96-well plates at 2000 cells/well (Costar; Corning, Corning, NY) for 24 hr and then exposed to various concentrations (0–40 μM) of imatinib for 72 hr. Cell proliferation was evaluated with the WST-8 [2-(2-methoxy-4-nitrophenyl)-3-(4-nitrophenyl)-5-(2,4-disulfophenyl)-2H-tetrazolium, monosodium salt] assay (Cell Counting Kit-SF; Nacalai Tesque) at the indicated post-treatment times. A microplate reader Model 680 (Bio-Rad Laboratories, Hercules, CA) was used to measure WST-8 absorption at a wavelength of 450 nm with a reference wavelength of 630 nm. Growth rate was expressed as the percentage of absorbance for treated cells vs. control cells. Experiments were performed in triplicate in two independent experiments, and the presented values are the averages of all six wells.

Apoptosis assay

GIST-T1 cells were seeded in 6-well plates at a density of 3×10^5 cells per well and treated with imatinib and/or TAG372 for 2 days. The cells were then washed with PBS, and caspase-3 activity was detected using the caspase-3 fluorometric assay kit (R&D systems, Minneapolis, MN) following the manufacturer's instructions. The presented values are the means of three independent experiments.

Statistical analysis

Statistical analyses were performed using the Mann–Whitney *U*-test or one-way analysis of variance (ANOVA), followed by Scheffe's test. One-way ANOVA followed by Dunnett's test was used for multiple comparisons.

Results

Quantitative phosphotyrosine proteomic analysis identifies upregulation of FYN and FAK in imatinib-exposed GIST-T1 cells

GIST-T1 cells that possessed the activating mutation in exon 11 of *KIT* are sensitive to imatinib, with a K_i value for imatinib of 20 nM. Time-dependent decreases in the tyrosine phosphorylation of KIT were observed when GIST-T1 cells were treated with 400 nM imatinib for 0, 1, 6 and 24 hr (Fig. 1*a*). These time-points were used for subsequent MS analysis, with 0 hr used as a control.

By utilizing immunoaffinity enrichment of phosphotyrosine peptides with quantitative phosphoproteomic analysis using iTRAQ technology combined with nano LC-MS/MS analysis, we identified 171 tyrosine phosphorylation sites spanning 134 proteins (Supporting Information Table S1). After imatinib treatment, a total of 11 phosphotyrosine sites spanning 11 proteins exhibited increases of >1.5-fold and 21 phosphotyrosine sites spanning 15 proteins showed decreases of <0.3-fold (Table 1). As a representative protein, we confirmed a dramatic decrease in the tyrosine phosphorylation levels of the KIT protein (Y609, Y703, Y747, Y823 and Y936). In contrast, imatinib induced increased phosphorylation of FYN (Y420) and FAK (Y576). Phosphorylation of FYN (Y420) upregulates tyrosine kinase activities, and phosphorylation of FAK (Y576) is critical for its maximal catalytic activity.

To validate these results obtained from iTRAQ analysis, we further examined the tyrosine phosphorylation of FYN and FAK using western blotting. As shown in iTRAQ analysis, western blotting confirmed that FYN (Y420) and FAK (Y576) were time dependently phosphorylated (Figs. 1*b* and 2*c*). When tyrosine phosphorylation in the activation loop was measured for other Src family kinases, we found that imatinib treatment did not increase tyrosine phosphorylation of SRC, LYN, LCK or YES (Fig. 1*b*).

Inhibition of FYN or FAK enhances imatinib sensitivity of GIST-T1 cells

To examine the functions of FYN in GIST-T1 cells exposed to imatinib, FYN expression was stably suppressed using a FYN shRNA plasmid. We cloned and established GIST-T1 B1, B2 and B3 cells, as well as GIST-T1 C cells transfected with empty vector as a control (Fig. 1*d*). Compared with GIST-T1 C cells, the FYN knockdown cell lines showed significantly decreased IC_{50} values for imatinib ($p < 0.05$; Fig. 1*d*).

We also examined the role of FAK activation in imatinib treatment. We repressed FAK expression using siRNA, and we used a FAK inhibitor (TAG372) to inhibit FAK phosphorylation. Transfection of FAK siRNA reduced IC_{50} values for imatinib ($p < 0.05$; Fig. 1*e*). When used with imatinib, TAG372 further decreased cell survival in a dose-dependent manner (Fig. 1*f*).

Inhibition of FAK improves imatinib sensitivity in GIST-T1-R cells

Next, we examined FAK activation in imatinib-resistant cell lines established from GIST-T1 cells. Eight imatinib-resistant cell lines were established by incubation of GIST-T1 cells with imatinib of gradually increased concentrations. Constitutive phosphorylation of FAK was observed in two imatinib-resistant

Short Report

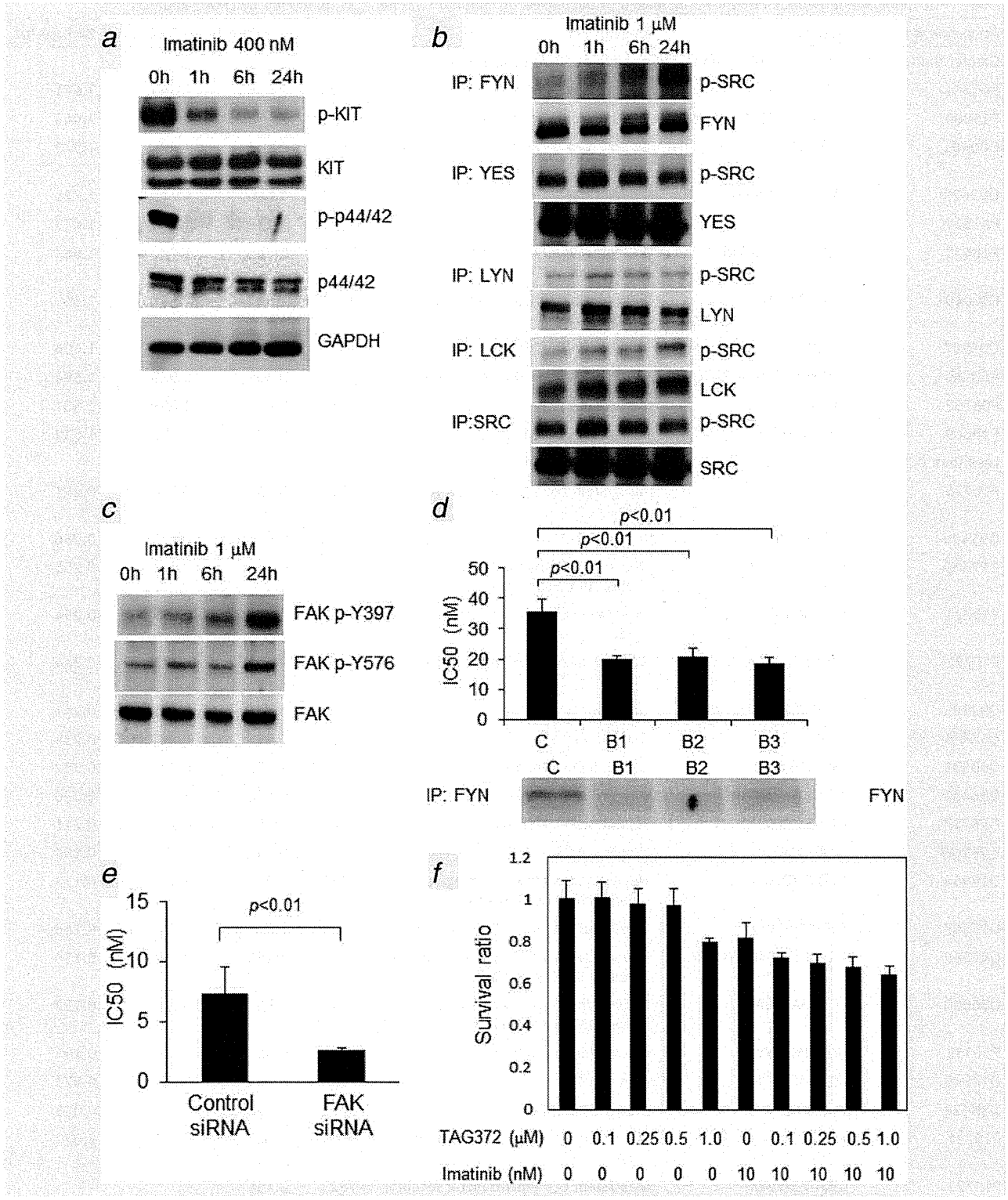

Figure 1. (*a*) Altered tyrosine phosphorylation levels detected by iTRAQ analysis were confirmed by western blotting. Imatinib treatment led to reduced phosphotyrosine levels. (*b*) Imatinib treatment changed SRC family kinase phosphorylation levels. (*c*) iTRAQ analysis showed that FYN (Y420) and FAK (Y576) exhibited similar tyrosine phosphorylation. (*d*) Compared with in GIST-T1 C cells, the IC_{50} for imatinib was significantly reduced in all FYN knockdown GIST-T1 cells (B1, B2 and B3). (*e*) The IC_{50} for imatinib was reduced in GIST-T1 cells that were transfected with FAK siRNA. (*f*) WST-8 assay showed the cell viability with imatinib and TAG372 treatment. Data are presented as means ± SD.

Table 1. Phosphotyrosine peptides that were increased or decreased by imatinib treatment, as quantified by iTRAQ analysis[1]

Accession Number	Sequence	Description	Site	1 hr/0 hr[2]	6 hr/0 hr[2]	24 hr/0 hr[2]
Greater than 1.5-fold increase of phosphorylated peptide at 24 hr compared with 0 hr						
P06241	LIEDNEYTAR	Tyrosine-protein kinase Fyn	Y420	0.845	2.365	3.641
P15880	AFVAIGDYNGHVGLGVK	40S ribosomal protein S2	Y133	2.138	1.807	2.443
O00401	VIYDFIEK	Neural Wiskott-Aldrich syndrome protein	Y256	0.768	1.491	1.978
Q99623	MLGEALSKNPGYIK	Prohibitin-2	Y248	1.446	1.778	1.726
P62829	NLYIISVK	60S ribosomal protein L23	Y38	2.138	1.348	1.679
P18433	VVQEYIDAFSDYANFK	Receptor-type tyrosine-protein phosphatase alpha	Y791	1.245	1.098	1.667
P30040	FDTQYPYGEK	Endoplasmic reticulum resident protein 29	Y64	1.804	2.558	1.640
Q05397	YMEDSTYYK	Focal adhesion kinase 1	Y570	1.043	0.893	1.606
A6NI28	LDTASSNGYQRPGSVVAAK	Rho GTPase-activating protein 42	Y792	0.599	0.980	1.594
P08758	LYDAYELK	Annexin A5	Y94	1.043	1.399	1.581
P18669	HYGGLTGLNK	Phosphoglycerate mutase 1	Y92	0.930	2.583	1.532
Less than 0.3-fold reduction of phosphorylated peptide at 24 hr compared with 0 hr						
P10721	IGSYIER	Mast/stem cell growth factor receptor Kit	Y747	0.649	0.244	0.291
O95490	SENEDIYYK	Latrophilin-2	Y1350	0.431	0.318	0.256
Q92569	LQEYHSQYQEK	Phosphatidylinositol 3-kinase regulatory subunit gamma	Y184	0.433	0.271	0.255
P10721	QEDHAEAALYK	Mast/stem cell growth factor receptor Kit	Y703	0.560	0.207	0.254
P10721	QISESTNHIYSNLANCSPNR	Mast/stem cell growth factor receptor Kit	Y936	0.445	0.212	0.244
Q92796	RDNEVDGQDYHFVVSR	Disks large homolog 3	Y673	0.556	0.427	0.241
Q5XXA6	STIVYEILKR	Anoctamin-1	Y251	0.508	0.720	0.235
Q00535	IGEGTYGTVFK	Cyclin-dependent kinase 5	Y15	1.877	0.821	0.232
Q06481	MQNHGYENPTYK	Amyloid-like protein 2	Y755	0.474	–[4]	0.220
O95297	INKSESVVYADIR	Myelin protein zero-like protein 1	Y263	0.785	0.249	0.211
Q969M3	QYAGYDYSQQGR	Protein YIPF5	Y42	0.145	–[4]	0.195
O14964	VVQDTYQIMK	Hepatocyte growth factor-regulated tyrosine kinase substrate	Y132	1.097	0.464	0.173
O95297	SESVVYADIR	Myelin protein zero-like protein 1	Y263	0.563	0.169	0.166
Q92569	VQAEDLLYGKPDGAFLIR	Phosphatidylinositol 3-kinase regulatory subunit gamma	Y373	1.186	0.176	0.130
O96000	YQDLGAYSSAR	NADH dehydrogenase [ubiquinone] 1 beta subcomplex subunit 10	Y143	0.864	0.393	0.122
P16333	LYDLNMPAYVK	Cytoplasmic protein NCK1	Y112	0.651	0.257	0.103
Q12846	NILSSADYVER	Syntaxin-4	Y251	0.179	0.131	0.072
Q8N128	YQYAIDEYYR	Protein FAM177A1	Y162	0.196	0.090	0.055
P10721	VVEATAYGLIK	Mast/stem cell growth factor receptor Kit	Y609	0.723	–[4]	0.023
P10721	DIKNDSNYVVK	Mast/stem cell growth factor receptor Kit	Y823	0.164	–[4]	–[4]
P53778	QADSEMTGYVVTR	Mitogen-activated protein kinase 12	Y185	1.582	0.888	–[4]

[1]The full list is provided in Supporting Information Table 1.
[2]The ratio of peptide derived from the iTRAQ reporter ion, as determined by iTRAQ analysis; 1 hr/0 hr, 6 hr/0 hr and 24 hr/0 hr refer, respectively, to the value of each peptide at 1, 6 and 24 hr divided by the value of that peptide at 0 hr.
[3]A 0-hr value of 0 (*i.e.* below background) and a positive value at 1, 6 or 24 hr.
[4]A 0-hr positive value and a value of 0 (*i.e.* below background) at 1, 6 or 24 hr.

GIST-T1 cell lines (GIST-T1-R2 and GIST-T1-R8), which had imatinib IC_{50} values of 30 μM, ~1000 times that of the GIST-T1 parent cells (Fig. 2*a*). TAG372 dose dependently inhibited FAK phosphorylation in GIST-T1-R2 (Fig. 2*b*), and significantly reduced the imatinib IC_{50} values when both drugs were used (Fig. 2*c*). Moreover, TAG372 induced apoptosis in GIST-T1-R2 (Fig. 2*d*). These results indicate that imatinib treatment induced activation of FYN and FAK in persistent GIST-T1 cells and was associated with imatinib insensitivity and resistance.

Discussion

Imatinib is a selective tyrosine kinase inhibitor of KIT, PDGFRA, ABL/BCR-ABL and CSF-1R, which was first used to treat GIST in 2000. Since then, it has been a standard treatment for advanced and/or recurrent GISTs.[6] Patients with advanced GIST usually respond to imatinib; however, most patients eventually experience disease progression with the reactivation of KIT tyrosine kinase and its downstream signaling pathways.[14,15] Although imatinib has high activity against GISTs, it cannot achieve complete eradication of tumor cells *in vivo* or *in vitro*. Results of the BFR14 trial showed that stopping imatinib treatment, even after complete response, resulted in disease progression or recurrence.[7,8] In chronic myelogenous leukemia (CML), mathematical models have indicated that secondary mutations might emerge after imatinib therapy;[16] therefore, residual tumor cells may also be a predisposing factor for acquired resistance to imatinib in GIST.

To quantitate the alteration of tyrosine phosphorylation levels induced by imatinib, we established quantitative tyrosine phosphoproteomic analysis. Using this technology, we identified 171 different tyrosine phosphorylation sites in 134 proteins of GIST-T1 cells. As we were searching for alternative pathways that were activated after inhibition of KIT signaling by imatinib, we pursued tyrosine kinases with increased tyrosine phosphorylation. Our comprehensive measures indicated that 11 tyrosine kinases exhibited tyrosine phosphorylation increases of greater than 1.5-fold (Table 1). The findings of the phosphoproteomic analysis were confirmed by western blotting showing the tyrosine-phosphorylation of KIT, FAK and other src-family kinases. SRC and LYN are reportedly phosphorylated and activated in GIST after imatinib treatment;[18] however, in the phosphoproteomic and western blotting analyses in the present study, we did not detect activation of SRC, LYN, YES, Lck or any other Src family kinases, except for FYN and FAK. Activation of FYN and FAK is reportedly involved in tumor proliferation and malignant transformation.[17–20]

FYN appears to participate in cell growth and survival, acting downstream of integrin and PI3K.[17,21] Although the

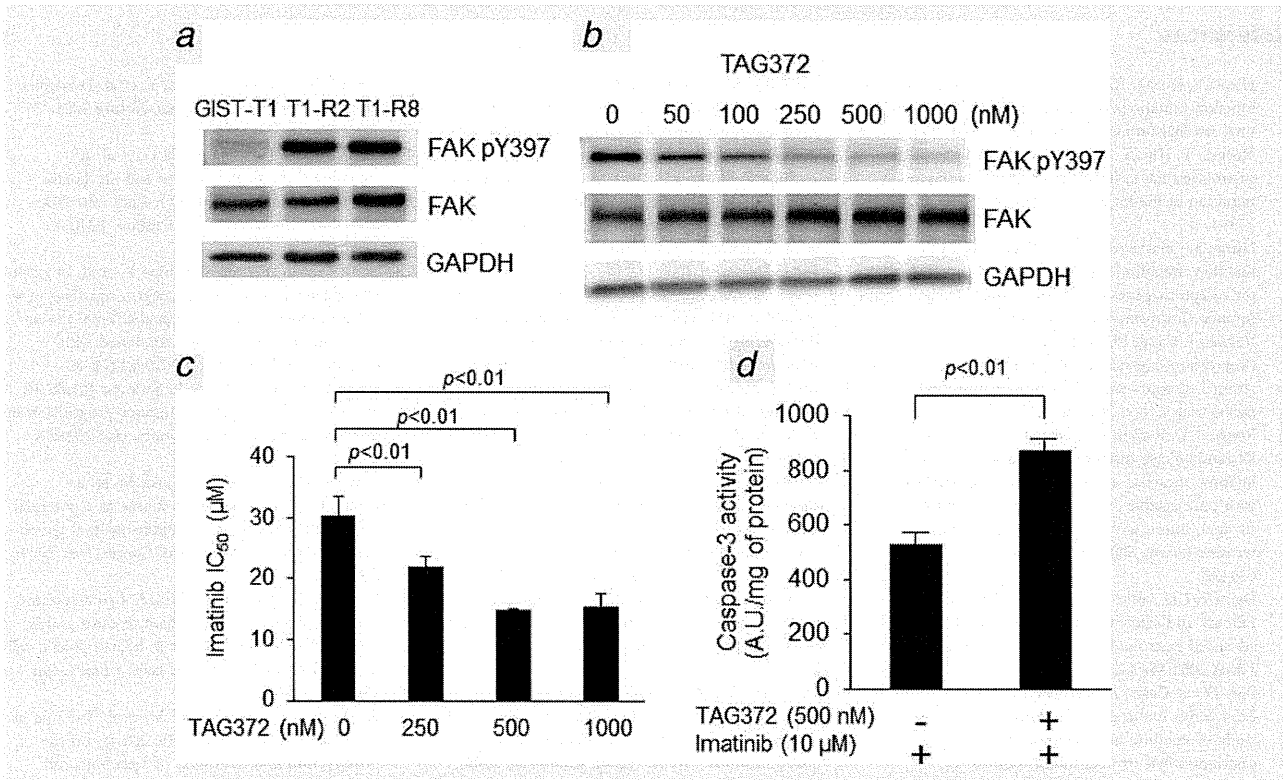

Figure 2. (*a*) Constitutive phosphorylation of FAK was observed in GIST-T1-R cells (GIST-T1-R2 and GIST-T1-R8). (*b*) Constitutive phosphorylation of FAK was observed in imatinib-resistant GIST-T1 cells (GIST-T1-R2), and TAG372 dose dependently inhibited this phosphorylation. (*c*) TAG372 reduced the IC_{50} of imatinib and induced apoptosis in GIST-T1-R2 cells. (*d*) TAG372 induced apoptosis in GIST-T1-R2 cells. Data are presented as means ± SD.

Short Report

shRNA silencing of FYN induced additional cell death in GIST-T1 cells during imatinib treatment, dasatinib (a SRC family kinase inhibitor) had no effect in combination with imatinib (data not shown). These results suggest the involvement of FYN in alternative survival signaling pathways.

FAK is also a nonreceptor tyrosine kinase that is activated through autophosphorylation at Tyr^{397} by integrin and growth factor receptors; this is followed by subsequent activation of other functional phosphorylation sites to transduce the signals to downstream pathways.[22,23] FAK is reportedly overexpressed in malignant GISTs and correlated with recurrence.[19] Furthermore, FAK phosphorylation is associated with imatinib-resistance of a KIT exon 17 mutation, but not exon 11 mutation.[20] This imatinib-resistance was diminished by TAE226, which inhibits FAK and insulin-like growth factor-1 receptor. Our findings showed that imatinib induced time-dependent FAK activation in GIST-T1 cells with an imatinib-sensitive mutation of KIT exon 11. Moreover, FAK inhibition using either a FAK-specific TAG372 inhibitor or siRNA decreased the viability of GIST-T1 cells under imatinib treatment. TAG372 also induced apoptosis in imatinib-resistant cell lines with FAK activation. Taken together, it appears that FAK activation may be a critical survival signal of GIST cells under imatinib treatment, and targeting FAK with imatinib may be a promising therapeutic approach.

When imatinib was removed, KIT was quickly rephosphorylated, and FYN and FAK were simultaneously dephosphorylated (data not shown), suggesting that alternative pathway activation is functional during imatinib treatment, and may not be accompanied with qualitative changes, such as new mutations. FYN inhibition was accompanied with a subsequent lack of FAK activation, while FAK inhibition resulted in increased FYN phosphorylation, thus indicating that FYN acted upstream of FAK. However, the critical changes that induce FYN activation and subsequent FAK phosphorylation remain unknown. Additional studies are required to elucidate the FYN activation mechanisms and the alternative pathways induced by imatinib, as well as their association with acquired drug resistance.

In summary, here we found that imatinib induced increased tyrosine phosphorylation of FYN and FAK in GIST-T1 cells. Blockade of these tyrosine kinases might be a potential target to overcome imatinib resistance. Additionally, iTRAQ-based quantitative phosphotyrosine-focused proteomic analysis appears to be a useful approach to screening for phosphoproteins associated with drug resistance.

Acknowledgments

This study was partly supported by grants from Novartis Pharmaceuticals.
Conflict of interest: N.T. has honoraria to disclose from the Novatis, Pfizer and Bayer within past 2 years.

References

1. Hirota S, Isozaki K, Moriyama Y, et al. Gain-of-function mutations of c-kit in human gastrointestinal stromal tumors. *Science* 1998;279:577–80.
2. Nishida T, Hirota S, Taniguchi M, et al. Familial gastrointestinal stromal tumours with germline mutation of the kit gene. *Nat Genet* 1998;19:323–4.
3. Hirota S, Ohashi A, Nishida T, et al. Gain-of-function mutation of platelet-derived growth factor receptor αgene in gastrtointestinal stromal tumors. *Gastroenterology* 2003;125:660–7.
4. Verweij J, Casali PG, Zalcberg J, et al. Progression-free survival in gastrointestinal stromal tumours with high-dose imatinib: randomised trial. *Lancet* 2004;364:1127–34.
5. Blanke CD, Rankin C, Demetri GD, et al. Phase III randomized, intergroup trial assessing imatinib mesylate at two dose levels in patients with unresectable or metastatic gastrointestinal stromal tumors expressing the kit receptor tyrosine kinase: S0033. *J Clin Oncol* 2008;26:626–32.
6. Demetri GD, von Mehren M, Blanke CD, et al. Efficacy and safety of imatinib mesylate in advanced gastrointestinal stromal tumors. *N Engl J Med* 2002;347:472–80.
7. Blay JY, Le Cesne A, Ray-Coquard I, et al. Prospective multicentric randomized phase III study of imatinib in patients with advanced gastrointestinal stromal tumors comparing interruption versus continuation of treatment beyond 1 year: the French Sarcoma Group. *J Clin Oncol* 2007;25:1107–13.
8. Le Cesne A, Ray-Coquard I, Bui BN, et al. Discontinuation of imatinib in patients with advanced gastrointestinal stromal tumours after 3 years of treatment: an open-label multicentre randomised phase 3 trial. *Lancet Oncol* 2010;11:942–9.
9. Nishida T, Shirao K, Sawaki A, et al. Efficacy and safety profile of imatinib mesylate (ST1571) in Japanese patients with advanced gastrointestinal stromal tumors: a phase II study (STI571B1202). *Int J Clin Oncol* 2008;13:244–51.
10. Mann M, Ong SE, Grønborg M, et al. Analysis of protein phosphorylation using mass spectrometry: deciphering the phosphoproteome. *Trends Biotechnol* 2002;20:261–8.
11. Rush J, Moritz A, Lee KA, et al. Immunoaffinity profiling of tyrosine phosphorylation in cancer cells. *Nat Biotechnol* 2005;23:94–101.
12. Taguchi T, Sonobe H, Toyonaga S, et al. Conventional and molecular cytogenetic characterization of a new human cell line, GIST-T1, established from gastrointestinal stromal tumor. *Lab Invest* 2002;82:663–5.
13. Yokoyama T, Enomoto T, Serada S, et al. Plasma membrane proteomics identifies bone marrow stromal antigen 2 as a potential therapeutic target in endometrial cancer. *Int J Cancer* 2013;132:472–84.
14. Nishida T, Kanda T, Nishitani A, et al. Secondary mutations in the kinase domain of the KIT gene are predominant in imatinib-resistant gastrointestinal stromal tumor. *Cancer Sci* 2008;99:799–804.
15. Antonescu CR, Besmer P, Guo T, et al. Acquired resistance to imatinib in gastrointestinal stromal tumor occurs through secondary gene mutation. *Clin Cancer Res* 2005;11:4182–90.
16. Michor F, Hughes TP, Iwasa Y, et al. Dynamics of chronic myeloid leukaemia. *Nature* 2005;435:1267–70.
17. Timokhina I, Kissel H, Stella G, et al. Kit signaling through PI 3-kinase and Src kinase pathways: an essential role for Rac1 and JNK activation in mast cell proliferation. *EMBO J* 1998;17:6250–62.
18. Rossi F, Yozgat Y, de Stanchina E, et al. Imatinib upregulates compensatory integrin signaling in a mouse model of gastrointestinal stromal tumor and is more effective when combined with dasatinib. *Mol Cancer Res* 2010;8:1271–83.
19. Koon N, Schneider-Stock R, Sarlomo-Rikala M, et al. Molecular targets for tumour progression in gastrointestinal stromal tumours. *Gut* 2004;53:235–40.
20. Sakurama K, Noma K, Takaoka M, et al. Inhibition of focal adhesion kinase as a potential therapeutic strategy for imatinib-resistant gastrointestinal stromal tumor. *Mol Cancer Ther* 2009;8:127–34.
21. Linnekin D, DeBerry CS, Mou S. Lyn associates with the juxtamembrane region of c-Kit and is activated by stem cell factor in hematopoietic cell lines and normal progenitor cells. *J Biol Chem* 1997;272:2745–55.
22. Serrels A, McLeod K, Canel M, et al. The role of focal adhesion kinase catalytic activity on the proliferation and migration of squamous cell carcinoma cells. *Int J Cancer* 2012;131:287–97.
23. Cox BD, Natarajan M, Stettner MR, et al. New concepts regarding focal adhesion kinase promotion of cell migration and proliferation. *J Cell Biochem* 2006;99:35–52.

Inhibition of angiopoietin 2 attenuates lumen formation of tumour-associated vessels *in vivo*

REI SUZUKI[1], HIROFUMI YAMAMOTO[1], CHEW YEE NGAN[1,2,3], MASAHISA OHTSUKA[1], KOTARO KITANI[1], MAMORU UEMURA[1], JUNICHI NISHIMURA[1], ICHIRO TAKEMASA[1], TSUNEKAZU MIZUSHIMA[1], MITSUGU SEKIMOTO[1], TOSHINARI MINAMOTO[2], YUICHIRO DOKI[1] and MASAKI MORI[1]

[1]Department of Surgery, Gastroenterological Surgery, Graduate School of Medicine, Osaka University, Suita, Osaka; [2]Division of Translational and Clinical Oncology, Cancer Research Institute, Kanazawa University, Kanazawa, Ishikawa, Japan

Received April 29, 2013; Accepted June 14, 2013

DOI: 10.3892/ijo.2013.2076

Abstract. Anti-angiogenic therapy, inhibition of a co-operative process with vascular endothelial cells and pericytes could be an effective strategy to treat malignant tumours. Apart from vascular endothelial growth factor (VEGF), angiopoietin 2 (Ang2) is a promising target of anti-angiogenic therapy. Although inhibition of Ang2 has been shown to decrease tumour size in preclinical and phase I trials, its mechanisms of action remain largely unknown. To elucidate the mechanisms of Ang2 inhibition, we have focused on differentiation of the vessels as well as on growth of the vessels, especially *in vivo*. LI-10, a selective Ang2 inhibitor was used. The *in vitro* effects of Ang2 inhibition or addition of Ang2 using HUVECs were also examined. Growth and differentiation of tumour-associated vessels were investigated in xenografts derived from a colon cancer treated by LI-10. Effects of VEGF inhibition were also examined to discriminate Ang2-specific action on the tumour-associated vessels. *In vitro* studies showed that VEGF enhanced proliferation and tube formation of HUVECs, and caused a significant increase in Rac1 and CDC42 expression when cultured in the collagen matrix gel, whereas neither Ang2 nor LI-10 affected *in vitro* behaviour of HUVECs or levels of the proteins. *In vivo*, on the other hand, we found that Ang2 inhibition with treatment of LI-10 dose-dependently decreased tumour growth. Furthermore, we found that LI-10 treatment extends the tumour-associated vessels whilst it suppressed a sound lumen formation. Histological analysis on xenografts suggests that Ang2 inhibition could have disturbed *in vivo* vascular differentiation. Our data provide a novel aspect that Ang2 may play an essential role in *in vivo* vascular differentiation, thus supporting a rationale for Ang2-targeted therapy against colon cancer.

Introduction

Angiogenesis, a co-operative process with vascular endothelial cells (ECs) and pericytes, is essential for tumour growth and expansion because the blood vessels supply malignant cells with sufficient oxygen and nutrition. Interruption of this process, therefore, could be an effective strategy for preventing malignant tumours. The putative angiogenic factor vascular endothelial growth factor (VEGF) is the best known to be involved in the growth and development of colorectal cancer (CRC) and its hepatic metastases (1-3). Anti-VEGF monoclonal antibody, bevacizumab (BV) is already clinically feasible in combination with conventional chemotherapies as the first anti-angiogenic drug that is proven to bring better prognosis of patients with colorectal cancer (CRC) in a phase III randomized controlled trial (4).

Besides VEGF, other important endothelial growth factors are angiopoietins (Angs), which are ligands for the endothelium-specific tyrosine kinase receptor Tie2 (5). Angs play a role in normal vascular development and in embryonic angiogenesis. Among 4 subtypes (Ang1, 2, 3 and 4), the best-characterized are Ang1 and its natural antagonist, Ang2. Ang1 is widely expressed in normal adult tissues, while Ang2 is expressed primarily at sites of vascular remodeling, such as the ovaries, uterus and placenta (5). Angiogenesis requires migration and remodeling of ECs derived from pre-existing blood vessels and regulation of the perivascular microenvironment. Thus, Ang2 destabilizes pre-existing vessels by weakening interactions between ECs and periendothelial supporting cells (PESCs) (3), also called vascular pericytes. Ang1 subsequently acts, via the Tie2 receptor, to remodel the primitive vessels and to help

Correspondence to: Dr Hirofumi Yamamoto, Department of Surgery, Gastroenterological Surgery, Graduate School of Medicine, Osaka University, 2-2 Yamadaoka, Suita, Osaka 565-0871, Japan
E-mail: hyamamoto@gesurg.med.osaka-u.ac.jp

Present address: [3]Joint Genome Institute, Walnut Creek, CA, USA

Abbreviations: Ang2, angiopoietin 2; CRC, colorectal cancer; EC, endothelial cell; VEGF, vascular endothelial growth factor; PBS, phosphate-buffered saline; RT-PCR, reverse transcription polymerase chain reaction

Key words: angiopoietin 2, vascular differentiation, lumen formation, vascular endothelial growth factor

maintain and stabilize mature vessels (6). Recent preclinical studies have shown that angiopoietin 2 may be another promising target against colon cancer through inhibition of either Ang2 (7-9) or Ang2+Angl (9,10).

There are two aspects of angiogenesis, i.e. growth and differentiation of the vessels. Although vascular growth (EC proliferation) has been examined by estimating vessel count and vessel size so far, little is known about vascular differentiation, i.e., vacuole or lumen formation, especially *in vivo*. In the present study, we investigated the effects of Ang2 on vascular growth and differentiation, *in vitro* and *in vivo*. We first examined *in vitro* effects of Ang2 inhibition or addition of Ang2 using HUVECs. Secondly we examined growth and differentiation of tumour-associated vessels when xenografts derived from a colon cancer were treated by the Ang2 inhibitor L1-10. Effect of VEGF inhibition was also examined to discriminate Ang2 specific action on the tumour-associated vessels. Our data provide a novel aspect that Ang2 may play an essential role in *in vivo* vascular differentiation, and therefore support a rationale for Ang2-targeted therapy against colon cancer.

Materials and methods

Cell lines. Human umbilical vascular endothelial cell (HUVEC) was purchased from Takara Bio Co. (Shiga, Japan). Human colon cancer cells (HCT116, DLD1, SW480) were purchased from the American Type Culture Collection (Manassas, VA). KM12SM (11) was a kind gift from Professor T. Minamoto (Cancer Research Institute, Kanazawa University, Kanazawa, Japan). Colon cancer cells were grown in DMEM supplemented with 10% fetal bovine serum (FBS), 100 U/ml penicillin, and 100 μg/ml streptomycin in 5% CO_2 at 37°C. HUVEC were grown on MCDB131 culture medium (Chlorella Inc., Tokyo, Japan) supplemented with 10% FBS, antibiotics, and 10 ng/ml basic fibroblast growth factor.

Attached collagen gel culture. HUVECs ($2x10^6$ cells/ml) were cultured on 0.03% type I collagen (Cellmatrix I-A, Nitta Gelatin Inc., Osaka, Japan) coated dishes. Collagen solution (0.3%) was diluted by Medium 199 (Life Technologies, Carlsbad, CA) and reconstruction buffer (50 mM NaOH, 260 mM $NaHCO_3$, 200 mM HEPES, according to the Nitta Gelatin manual). After collagen coating, cell suspension was seeded, then medium containing appropriate concentration of reagent such as VEGF, Ang2 and L1-10 was added, and 24 h later, same volume of PBS, 1/25 volume of Collagenase N-2 (Nitta Gelatin Inc.) solution were added into the well, incubated at 37°C with mild shaking. Suspension was spun down, pellet was resuspended with same volume of PBS and 1/50 volume of Collagenase N-2. After 10 min incubation at 37°C, pellet was lysed and supernatant was used for western blot analysis (12).

Collagen gel matrix culture. In vitro formation of tubular structures by HUVEC was examined using collagen gel matrix culture. Collagen gel (0.06%) layer was made (base layer). Collagen gel (0.06%) suspended with HUVECs was added onto base layer, and immediately polymerized at 37°C. Medium containing appropriate concentration of reagent such as VEGF, Ang2 or L1-10 was added. Twenty-four or 48 h later, HUVECs were harvested as mentioned above or observed under an inverted microscope. Cell concentration of HUVECs for western blot analysis and morphogenesis were $1x10^6$ cells/ml and $3x10^6$ cells/ml, respectively.

Reagents and antibodies. Human recombinant VEGF and mouse IgG was obtained from IBL Co. Ltd. (Gunma, Japan). Ang2 was purchased from (R&D Systems, Minneapolis, MN). The following antibodies were used at appropriate concentrations as recommended by the manufacturers: antibodies for angiopoietin 2 (C-19, Santa Cruz Biotechnology, Santa Cruz, CA), VEGF (A20, Santa Cruz Biotechnology), Tie2 (H-176 for immunoprecipitation, C-20 for western blot analysis, Santa Cruz Biotechnology), phosphorylated Tie2 (Tyr992, #4221, Cell Signaling Technology, Danvers, MA), actin (Sigma-Aldrich, St. Louis, MO), Racl (Cytoskeleton, Denver, CO), CDC42 (BD Biosciences, San Jose, CA), CD31 and α smooth muscle actin (Dako, Glostrup, Denmark).

L1-10. L1-10, an Ang2 neutralizing peptibody (genetically-engineered peptide-Fc fusion protein) was kindly donated by Amgen Inc. (Seattle, WA). L1-10 is a specific inhibitor of angiopoietin-2, and inhibits interactions between Tie2 in endothelial cells and human or mouse angiopoietin-2 (7,13,14).

Binding activity of L1-10 to Ang2 was measured by ELISA. Recombinant human angiopoietin-2 (R&D Systems) was immobilized on a plate. After blocking with 1% BSA, 1 pM recombinant human Tie2/Fc Chimera (R&D Systems) was added, from 500 to 0.02 nM of L1-10 and recombinant human IgG1 Fc (R&D Systems). Molecular weight of L1-10 was assumed as 62.5 kDa and that of IgG Fc was 26.6 kDa. Anti-Tie2 monoclonal antibody (BD Biosciences) at 0.25 μg/ml was added. After washing, 0.05 μg/ml anti-mouse IgG (Goat IgG) Fab' conjugated with HRP (IBL Co. Ltd.) was added. Color development was done by incubating with tetramethyl benzidine solution for 30 min. Absorbance at 450 nm was measured by microplate reader.

Western blot analysis. Western blot analysis was performed as we described previously (12). Briefly, the protein samples (25 μg) were separated by 10 or 12.5% PAGE followed by electroblotting onto a polyvinylidene difluoride (PVDF) membrane. The membrane was incubated with the primary antibodies at the appropriate concentrations (1:100 for Ang2, 1:200 for VEGF and Tie2, 1:250 for CDC42 and 1:1,000 for Racl actin and phosphorylated Tie2). The protein bands were detected using the Amersham enhanced chemiluminescence detection system (GE Healthcare, Buckinghamshire, UK).

To detect phosphorylated Tie2, lysates of HUVEC were immunoprecipitated with an anti-Tie2 antibody (H-176, Santa Cruz Biotechnology). Immunocomplexes were recovered on Protein A-Sepharose (GE Healthcare) and separated by SDS-PAGE, transferred to blotting membrane as described above, then probed with anti-phosphorylated Tie2 antibody (#4221, Cell Signaling Technology).

Measurement of Ang2 and VEGF secretion in culture medium. Each cell line was cultured until about 70% confluence in DMEM supplemented with FBS. The medium was then

Table I. Administration schedules of combination treatment.

Group	Drug	Route	Interval (days)	Dose	
				Early	Late
Control	IgG	i.p.	3	200 μg	150 μg
VEGF	Anti-VEGF antibody	i.p.	3	200 μg	150 μg
Combination	Anti-VEGF antibody	i.p.	3	200 μg	150 μg
	L1-10	s.c.	2	5 mg/kg	10 mg/kg

replaced with new medium without FBS, collected 24 h later, and stored at -80°C. Ang2 and VEGF levels were analyzed using the QuantikineHuman Angiopoietin-2 immunoassay kit (R&D Systems) and the Human VEGF assay kit (IBL Co. Ltd.), respectively.

Animals. Female 4-week-old athymic nude mice were purchased from Nihon CREA Inc. (Tokyo, Japan) and were housed under pathogen-free conditions in microisolator cages with irradiated rodent chow and water available *ad libitum*. The experimental protocol was approved by the Ethics Review Committee for Animal Experimentation of Osaka University School of Medicine.

Subcutaneous xenograft model. The most actively secreting VEGF and Ang2 cell line was KM12SM. KM12SM cells at 80-90% confluence was used in experiments. A total of $1x10^6$ cells ($5x10^6$ cells/0.1 ml DMEM without FBS) was subcutaneously inoculated in the right flank of each mouse. The doses of each drug were based on the results of preliminary experiments. Mice were randomly assigned to the groups.

Single agent treatment: L1-10 or anti-VEGF antibody treatment was started immediately after inoculation. There were four mice in each group. L1-10 was administered subcutaneously into the left flank skin at 2 mg/kg, 5 mg/kg every two days. Anti-VEGF antibody (200 μg, IBL Co. Ltd.), was administered intraperitoneally every three days. Control groups for each drug were administered mouse immunoglobulin (IgG) in the same manner as the experimental group. Treatment was continued for 18 days. Mice were sacrificed at day 20, and tumours were harvested for histological examinations.

Combination treatment with early administration: L1-10 and anti-VEGF antibody injections were initiated immediately after inoculation. There were five mice in each group. Anti-VEGF antibody (200 μg) was administered intraperitoneally every three days. Combination group was administered 5 mg/kg of L1-10 subcutaneously every two days and 200 μg of anti-VEGF antibody was administered intraperitoneally every three days. Control group was administered 200 μg of mouse IgG intraperitoneally every three days. Treatment was continued to day 18. Mice were sacrificed at day 20, and tumours were harvested for histological examinations.

Combination treatment with late administration: L1-10 and anti-VEGF antibody treatment were initiated 5 days after inoculation. There were four mice in each group. Dose was 10 mg/kg for L1-10, 150 μg for anti-VEGF antibody, 150 μg for IgG, and combination (L1-10 and anti-VEGF antibody) treatment was applied. Treatment was continued to day 31. At day 34 mice were sacrificed.

After inoculation of KM12SM cells into nude mice, control IgG, anti-VEGF antibody and L1-10 were administered as summarized in Table I.

Evaluation of antitumour activity. Tumour size and body weight were measured every two days. Tumour size was measured by an electronic caliper. Tumour volume was calculated according to the following formula: length (mm) x width^2 (mm)/2. Mice were sacrificed at the final day of experiment. Gross autopsy findings were noted.

Immunohistochemistry. Immunostaining was done as described previously (3). Briefly, after deparaffinization, heat antigen retrieval was done in 10 mM citrate buffer (pH 6.0) at 95°C for 40 min. The slides were then processed for immunohistochemistry using the Vectastain Elite avidin-biotin complex kit (Vector Laboratories, Burlingame, CA). Primary antibodies were applied to sections at a dilution of 1:750 for CD31 and incubated overnight at 4°C. For the negative control, non-immunized immunoglobulin G (Vector Laboratories) was used as a substitute for the primary antibody.

Double-staining of endothelial cells and pericytes was performed with anti-CD31 antibody and anti-α-SMA antibody, respectively. First, CD31 staining which yields a brown color was performed. After removal of the CD31 antibody by thorough washing in 0.1 M glycine solution (pH 2.2) for 1 h, mouse monoclonal anti-human SMA antibody at a dilution of 1:200 was applied to the section for 2 h at room temperature. This step was followed by incubation with anti-mouse secondary antibody conjugated with a dextran backbone containing alkaline phosphatase (EnVision AP; Dako) for 30 min. Color development (deep pink) based on alkaline phosphatase activity was achieved using fuchsin solution.

Image analysis. CD31-stained samples were used for image analyses. Outer and inner contours of vessels at 100-times magnification in one microscopic field were measured with WinROOF program Ver.5.5.0 (Mitani Corporation, Fukui, Japan). Outer contours were expressed as surface area of vessel and inner contours were expressed as surface area of lumen.

Statistical analyses. Data are expressed as mean ± SD. Statistical analysis was performed using the StatView J-4.5 program (Abacus Concepts Inc., Berkeley, CA). The mean

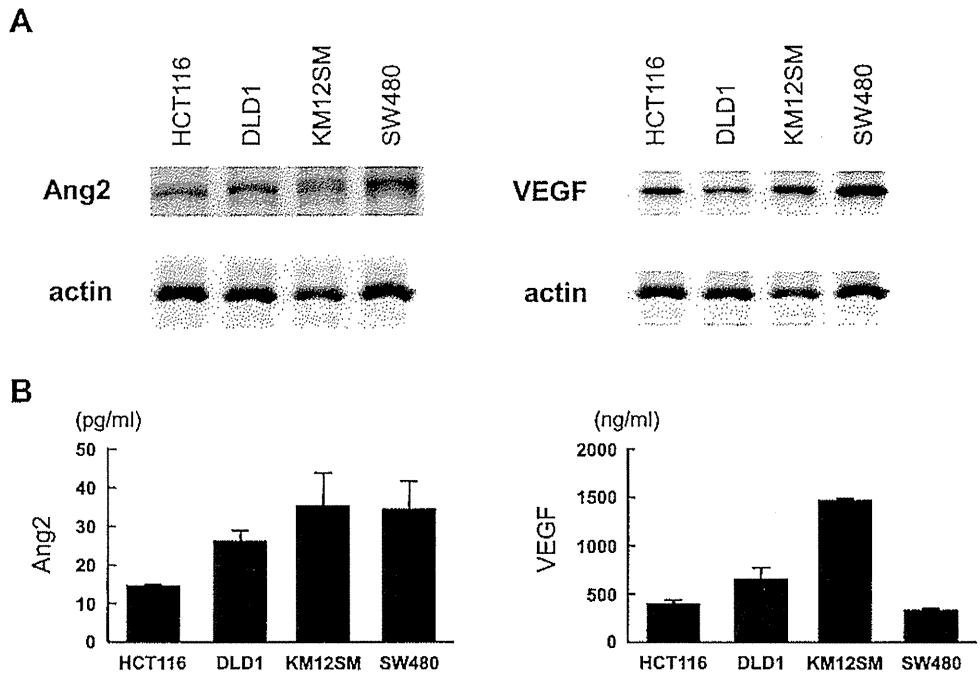

Figure 1. (A) Expression of Ang2 (83 kDa) and VEGF (42 kDa) in colon cancer cell lines. The colon cancer cell lines displayed intense expression of Ang2 and VEGF. Actin bands (42 kDa) served as a loading control of equal amount of the protein lysate. (B) Measurement of Ang2 and VEGF levels in the cultured medium. ELISA showed various levels of Ang2 and VEGF in the culture medium of each colon cancer cell line. KM12SM was found to release high level of both Ang2 and VEGF into the medium. Data are expressed as mean ± SD from triplicate cultures.

tumour volume of each treatment group was compared by Student's t-test. A p-value <0.05 was considered statistically significant.

Results

Ang2 and VEGF expression in colon cancer cells. Western blot analysis showed that HCT116, DLD1, KM12SM and SW480 colon cancer cell lines exclusively displayed intense expression of both Ang2 and VEGF (Fig. 1A). ELISA showed various levels of Ang2 and VEGF in the culture medium and KM12SM was found to release high level of both Ang2 and VEGF (Fig. 1B).

Inhibition of binding affinity between Ang2 and Tie2 by L1-10 peptibody. In vitro immunoreaction test indicated that the L1-10 peptibody (L1-10) blocked the binding of Ang2 and Tie2 at more than 0.1 nM in a dose-dependent manner, while addition of human IgG1 Fc at various concentrations did not affect Ang2-Tie2 binding affinity (Fig. 2A). To examine the activation status of the Tie2 receptor, phosphorylation on Tyr992 of the Tie2 receptor was examined using the HUVEC with early exposure (15 min) by Ang2 or L1-10. Although Tie2 expression did not change, Ang2 inhibited phosphorylation of Tie2 receptor at 200 ng/ml. This dephosphorylation by Ang2 was abolished with addition of L1-10 at 30 ng/ml. (Fig. 2B).

Effects of VEGF, Ang2 and L1-10 on growth and tube formation of HUVECs. Addition of Ang2 or L1-10 did not enhance cell proliferation and tube formation of HUVECs (Fig. 3A and B, upper panels). On the other hand, addition of VEGF at 25 ng/ml enhanced growth and it resulted in increased number of tube formation of HUVECs (Fig. 3A and B, lower panels).

We then examined protein expression of Rac1 and CDC42 since these molecules are reportedly shown to be involved in process of tube formation of HUVECs (15,16). As shown in Fig. 3C, VEGF enhanced expression of both the Rac1 and the CDC42 proteins, while Ang2 at various concentrations did not affect the expression of the two proteins (Fig. 3C).

Ang2 inhibition by L1-10 treatment reduced tumour formation in nude mice. Subcutaneous injection of L1-10 (at 2 mg/kg or 5 mg/kg) into different sites of KM12SM xenografts inhibited tumour formation dose-dependently (Fig. 4A). In the 5 mg/kg group, tumour formation was significantly inhibited from day 10 compared to that of control group. In the 2 mg/kg group, tumour formation was inhibited in later phase of experiment period. Histopathological examination of xenografts revealed that when compared to control IgG treatment (Fig. 4Ba), tumour vessels in L1-10 treated mice extended like a pine needle and lumen formation was scarcely noted (Fig. 4Bb). Double staining for CD31 and α-SMA showed that vascular endothelial cells were tightly covered with pericytes in L1-10 treated group, whereas only partial recruitment of pericytes was found in the control group. In treatment with VEGF neutralizing antibody, tumour vessels decreased and endothelial cells were relatively covered with pericytes (Fig. 4Bc).

Image analysis for lumen formation. To evaluate lumen formation in each treatment, the contour of vessel or lumen was traced using the image analysis software, and the vessel area and the lumen area was estimated as described in Materials

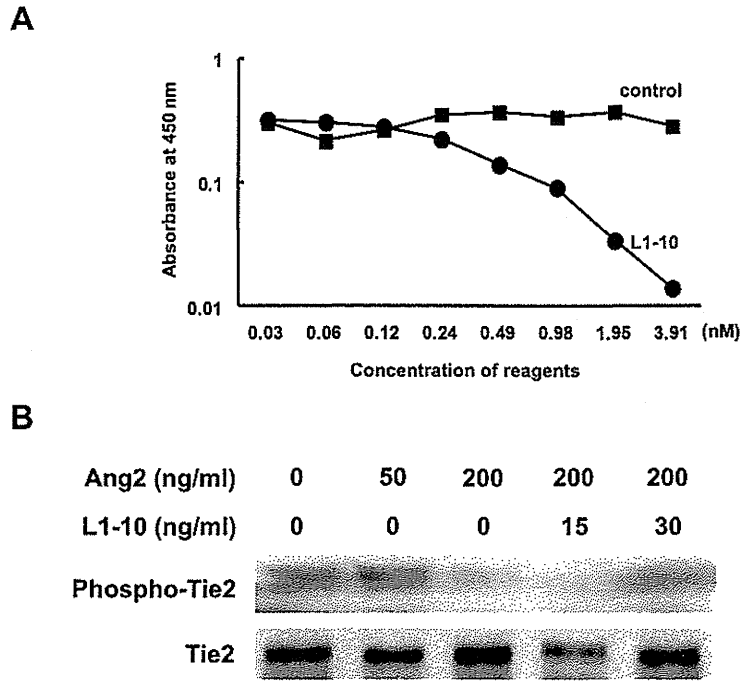

Figure 2. (A) Inhibition of binding affinity between Ang2 and Tie2 by L1-10 peptibody. Immunoreaction between recombinant human Ang2 and recombinant human Tie2 Fc Chimera was measured by tracing Tie2 amount in the Ang2-Tie2 complex in 96-well plates. L1-10 decreased binding affinity of Ang2 and Tie2 at more than 0.1 nM dose-dependently, while addition of human IgG1 Fc at various concentrations did not affect Ang2-Tie2 binding. (B) Tie2 phosphorylation status on Tyr992 of Tie2 was examined. HUVEC were treated by Ang2 alone (lanes 2 and 3) or Ang2 and L1-10 (lanes 4 and 5) at the indicated concentration for 15 min at 37°C. Cell lysates were immunoprecipitated using anti-Tie2 antibody. Ang2 inhibited phosphorylation of Tie2 at 200 ng/ml and L1-10 at 30 ng/ml recovered inhibition of phosphorylation by Ang2. Molecular weight of both Tie2 and phosphorylated Tie2 was 140 kDa.

and methods. Treatment with anti-VEGF antibody significantly decreased both vessel area and lumen area ($p<0.01$ for both, Fig. 5A and B). On the other hand, L1-10 treatment at 5 mg/kg did not decrease vessel area (Fig. 5A), but it significantly decreased the lumen area ($p<0.01$, Fig. 5B). When the ratio of lumen area to vessel area was calculated, there was a significant decrease in L1-10 treatment group ($p<0.01$, Fig. 5C).

Combination treatment. Since the histopathological analysis indicated that inhibition of either Ang2 or VEGF showed different anti-vascular effect, we examined whether the two treatments would produce enhanced tumour inhibitory effects. After inoculation of KM12SM cells into nude mice, control IgG, anti-VEGF antibody, and L1-10 were administered as summarized in Table I.

Combination treatment with anti-VEGF and L1-10 administered from the day of inoculation significantly decreased tumour volume compared to anti-VEGF treatment except days 8 and 10 (Fig. 6A). When treatment started 5 days after inoculation, combination treatment showed no significant difference compared to anti-VEGF treatment (Fig. 6B).

Discussion

In this study, we found Ang2 inhibition exerts a superb efficacy especially *in vivo*. Histological analysis on xenografts planted in nude mice suggests that Ang2 inhibition could have disturbed *in vivo* vascular differentiation, i.e., lumen formation. There are two important aspects on tumour angiogenesis, that is, growth of vascular endothelial cells and vascular differentiation. Compared to regulation of vascular endothelial cell growth, the underlying mechanism on vascular differentiation remains largely unknown. About three decades ago, Folkman and Haudenschild observed vacuoles that penetrate from one endothelial cell to another one by *in vitro* system (17). Subsequent *in vitro* investigation gradually revealed that pinocytosis occurs via interaction of integrin-extracellular matrix through CDC42 or Rac1-dependent manner (18,19). It was also demonstrated that several vacuoles, generating at 2-4 h in a single HUVEC, undergo intra-cellular fusion, and later at 24-48 h HUVECs make assembly body, resulting in lumen formation, raising VE cadherin as a molecular basis (20). By contrast, *in vivo* lumen formation has not been assessed for a long time because direct observation is rather difficult on the process of lumen formation that occurs profoundly in the animal body. *In vivo* tube formation of the vascular endothelial cells was reported for the first time in 2006, through observation of zebrafish by two-photon imaging system (21).

In this study, we employed L1-10 peptibody, the Ang2 selective inhibitor that showed 1,000-fold inhibitory selectivity for Ang2 over Ang1 (7,13,14). We confirmed by ELISA that L1-10 abolished *in vitro* binding affinity between Ang2 and Tie2 in a dose-dependent manner (Fig. 2A).

We further confirmed that phosphorylation at Tyr992 of Tie2 receptor, which had undergone dephosphorylation by stimulation with the recombinant Ang2, is rescued by the addition of L1-10. (Fig. 2B). These data indicate that L1-10 indeed blocks Ang2-Tie2 signal transduction.

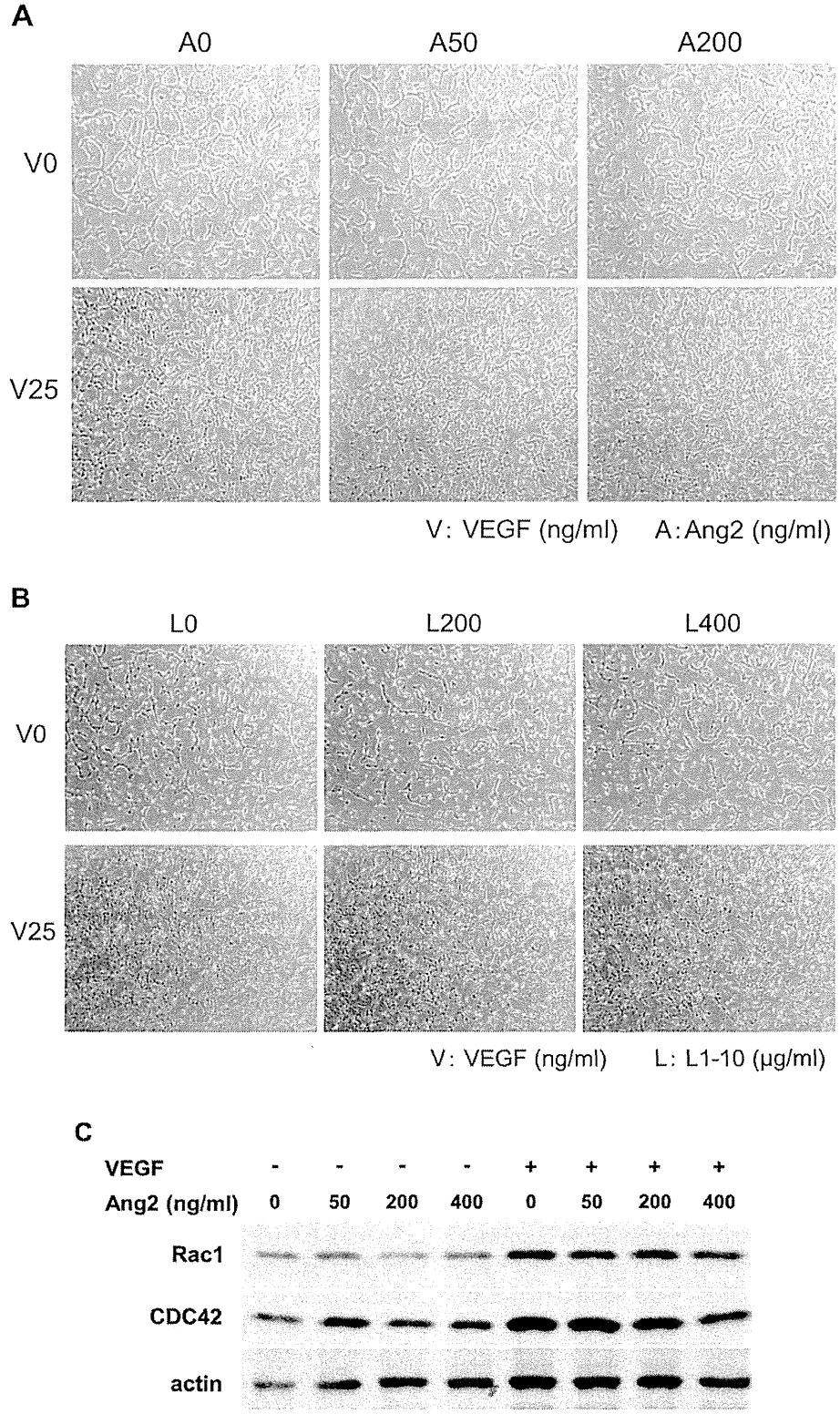

Figure 3. *In vitro* growth and tube formation of HUVECs. (A) Addition of Ang2 (at 50 and 200 ng/ml) or (B) L1-10 (at 200 and 400 μg/ml) for 72 h did not affect behaviour of HUVECs when cultured in the collagen matrix, in the absence of VEGF (V0). On the other hand, addition of VEGF at 25 ng/ml (V25, lower panels) enhanced cell proliferation and resulted in increased number of tube formation of HUVECs. (C) Protein expression of Rac1 (21 kDa) and CDC42 (22 kDa) after treatment of VEGF or Ang2 for 48 h. VEGF treatment at 25 ng/ml enhanced expression of both Rac1 and CDC42, while Ang2 at various concentrations did not affect the expression of the two proteins.

Previous reports on Ang2 inhibition in tumour cells showed decreased tumour volume. These studies used the Colo205 colon cancer cells (7-10,22,23) and other colon and breast cancer cells (8), the LuCap23.1 prostatic cancer cells (13) and U-87 glioma cells (24). The KM12SM colon cancer cells employed display high levels of Ang2 and VEGF among

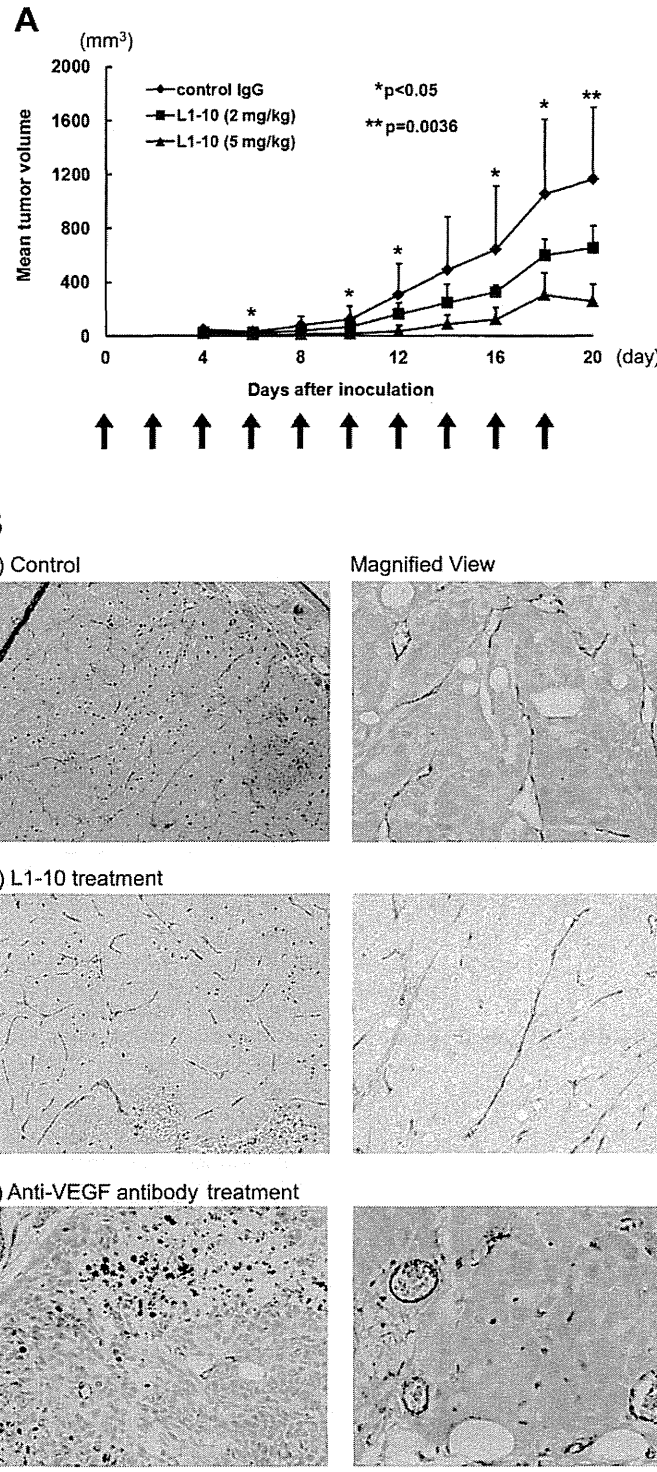

Figure 4. Growth curve of KM12SM xenograft model. (A) Subcutaneous injection of L1-10 (at 2 or 5 mg/kg) into different sites of KM12SM xenografts inhibited tumour formation in a dose-dependent manner. (B) Histopathological examination of xenografts (a) control IgG treatment, (b) L1-10 treatment, (c) treatment with anti-VEGF neutralizing antibody. Anti-VEGF antibody was administered into peritoneal cavity at 200 μg on days 0, 3, 6, 9, 12, 15 and 18. Mice were sacrificed on day 20. Double staining for CD31 (brown) and α-SMA (pink) was performed to label vascular endothelial cells and vascular pericytes, respectively. Magnifications (left panel, right panel): (a) x100, x400; (b) x100, x200; and (c) x200, x400.

several CRC cells (Fig. 1) and produced abundant tumour vessels in xenografts (Fig. 4). Moreover, the KM12SM cells were initially isolated as highly metastatic cells that develop marked spontaneous metastasis to liver (11) and shown to be highly activated state in β catenin/TCF oncogenic pathway (25,26). We considered that this cell type with such aggressive features could be a suitable material in evaluation of superb efficacy of Ang2-targeted therapy.

In vitro studies showed that VEGF enhanced proliferation and tube formation of HUVECs, and caused a clear increase in Rac1 and CDC42 expression when cultured in the collagen matrix, whereas neither Ang2 nor L1-10 affected *in vitro*